UNIVERSITY OF NAPLES FEDERICO II

DOCTORATE
MOLECULAR MEDICINE AND MEDICAL BIOTECHNOLOGY

XXX CICLO

Selection of aptamers targeting a hypoxia marker: Carbonic Anhydrase-IX (CA-IX)

Tutor
Dott. Vittorio de Franciscis

Candidate
Silvia Nuzzo

COORDINATOR

Prof. Vittorio Enrico
Avvedimento

Academic Year 2016/2017

“Selection of aptamers targeting a hypoxia marker: Carbonic Anhydrase-IX (CA-IX)”

TABLE OF CONTENTS

LIST OF PUBLICATIONS

1. Esposito CL, **Nuzzo S.**, CatuognoS., Romano S., de NigrisF., de FranciscisV. STAT3 gene silencing by Aptamer-siRNA chimera as selective therapeutic for Glioblastoma. Under revision to MolTherNucleic Acids.
2. Iaboni M, Fontanella R, Rienzo A, Capuozzo M, **Nuzzo S**, Santamaria G, Catuogno S, Condorelli G, de Franciscis V, Esposito CL. Targeting Insulin Receptor with a Novel Internalizing Aptamer. Mol Ther Nucleic Acids. 2016 Sep 20;5(9):e365. doi: 10.1038/mtna.2016.73.
3. Esposito CL, **Nuzzo S**, Kumar SA, Rienzo A, Lawrence CL, Pallini R, Shaw L, Alder JE, Ricci-Vitiani L, Catuogno S, de Franciscis V. A combined microRNA-based targeted therapeutic approach to eradicate glioblastoma stem-like cells. J Control Release. 2016 Sep 28;238:43-57. doi: 10.1016/j.jconrel.2016.07.032. Epub 2016 Jul 21.

ABBREVIATIONS:

2’-F-Py, 2′-Fluoro pyrimidine

2’NH2-Py, 2’-amino pyrimidine

ELISA, enzyme-linked immunosorbent assay

FDA, Food and Drug Administration

99mTc, Technetium-99m

SELEX, Systematic Evolution of Ligands by Exponential enrichment

mTOR, mammalian target of rapamycin

Akt, Protein Kinase B

CAs, Carbonic anhydrases

CA-IX, carbonic anhydrase IX

HIF-1, Hypoxia Inducible Factor 1

ROS, reactive oxygen species

PHD, oxygen-dependent prolyl-4-hydroxylase domain

pVHL, von Hippel–Lindau tumour suppressor protein

pHe, extra-cellular pH

MAPK, Mitogen-activated protein kinases

PI3K, Phosphatidylinositol-4,5-bisphosphate 3-kinase

VEGF, vascular endothelial growth factor

GLUT1/3, Glucose transporter 1/3

MMPs, Matrix metalloproteinases

IGF-2, Insulin-like growth factor 2

TGF-α, Transforming growth factor alpha

PG, a proteoglycan-like domain

TM, transmembrane region

IC, cytoplasmic tail

LDH5, Lactate dehydrogenase 5

MCT4, Monocarboxylate transporter 4

VHL, Von Hippel–Lindau

ABSTRACT

Carbonic anhydrases (CAs) family are metalloenzymes, involved in pH control, catalysing the reversible conversion of carbon dioxide to protons and bicarbonate. Until now, 16 isoenzymes have been identified with different tissue distribution, subcellular localization and molecular biophysical properties.
Among them, carbonic anhydrase IX (CA-IX) is a hypoxic marker because the master regulator of hypoxia, named Hypoxia Inducible Factor 1 (HIF-1), promotes its expression.
Thanks to its catalytic activity, CA-IX reduces extracellular pH. The acid microenvironment increases cancer cell proliferation and invasion, giving to CA-IX an important role during the cancer progression.
Unlike other CAs, many studies have demonstrated that CA-IX is expressed only in few normal tissues, whereas it becomes overexpressed in many types of cancer. Therefore, the targeting of CA-IX, using specific tools, opens new important fields to improve the conventional therapies and the early diagnosis in cancer.
Based on these evidences, we would generate new strategies able to target CA-IX. To this end, nucleic acid-based aptamers are emerging as new tools perfectly suitable to different fields.
Aptamers are selected by an *in vitro* combinatorial chemistry approach, named Systematic Evolution of Ligands by Exponential enrichment (SELEX), and they are able to bind with high affinity and specificity virtually any given molecule. Compared to monoclonal antibodies, they have a small size that results in their rapid tumour penetration; they are not immunogenic and could be easily modified to increase their *in vivo* stability.
Thus, in this study we describe the selection of RNA-based aptamers directed against the extracellular domain of CA-IX.
Firstly, we performed two different cell-based SELEX protocols that allowed the enrichment for CA-IX specific aptamers.
Furthermore, we characterized and improved the two best sequences selected, named S-47s1 and S-51s1, that we are still studying to handle a final product usable for diagnostic and therapeutic purposes.

1. BACKGROUND

1.1 Hallmarks of cancer

Cancer is a class of diseases characterized by out-of-control cell growth [1].
It is the second leading cause of death in the world after cardiovascular diseases.
By the mid-1980s, since when researchers defined genomic alterations (nucleotide substitutions, chromosomal copy number alterations, and DNA rearrangements) [2] of two principal cancer-causing genes, named oncogenes and tumour suppressor genes , lot of new progresses have been made to better understand the molecular basis of the cancer.
In 2000, Hanahan and Weinberg proposed six hallmarks of cancer to clarify how the normal cells can progressively evolve to a neoplastic phenotype.
They postulated that cells become able to acquire a succession of hallmark capabilities (sustaining proliferative signalling, evading growth suppressors, activating invasion and metastasis, enabling replicative immortality, inducting angiogenesis, resisting to cell death), that improve their tumorigenesis and malignancy [3]
In 2010, always Hanahan and Weinberg added other two emerging hallmarks [4]:

- the capability to modify the cellular metabolism to support neoplastic proliferation.
- the capability of cancer cells to evade immunological response, in particular by T and B lymphocytes, macrophages, and natural killer cells.

In the last few years, as Caroline Wigerup shows (Fig.1), the eight hallmarks seems to be regulated by tumour hypoxia including cell proliferation, apoptosis, altered metabolism, immune responses, genomic instability, vascularization, invasion and metastasis [5].
Thus, the linkage emerged between the hypoxic condition and cancer could represent a new prognostic/predictive markers to improve the conventional therapies and to improve the early diagnosis of the cancer.

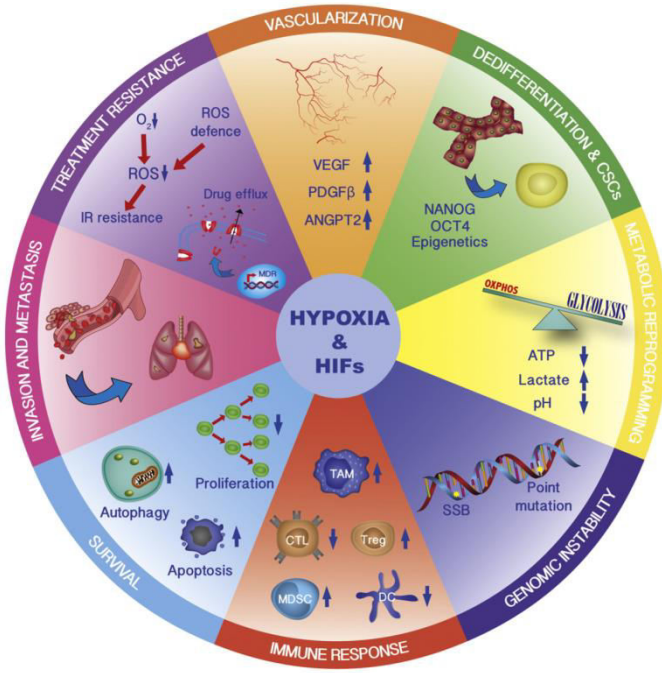

Fig.1: **Hypoxia and HIFs regulate hallmarks of cancer and multiple cancer phenotypes.** The hypoxia regulates treatment resistance, vascularization, dedifferentiation, genomic instability, survival, immune response, invasion and metastasis. (From Wigerup C. et al. 2016)

1.2 Hypoxia in cancer

Hypoxia generally refers to sub-physiologic tissue oxygen levels (5–10 mmHg), *versus* 40–60 mmHg in healthy tissues [6].
The interruption of vascular supply or the cell proliferation outstrips neoangiogenesis promotes hypoxia.
Three types of hypoxia exist:

- Diffusion-related (chronic): the hypoxia is caused by an increase in diffusion distances with tumour expansion;
- Perfusion-related (acute): hypoxia is caused by insufficient blood flow;
- Anaemic: the hypoxia is caused by a decrease in oxygen transport capacity [7].

In 1955, Thomlinson and Gray postulated the origin of chronic hypoxia in human tumours [8], whereas, acute hypoxia was presented by Brown and colleagues in 1979 [9].
The oxygen used by cells close to vessels leaves inadequate oxygen for the cells further away from the vessels (100 ml of capillary blood vessels) causing the process called "chronic hypoxia" [10].
The process produces long-term cellular changes, such as high frequency of DNA breaks, accumulation of DNA replication errors, potentially leading to genetic instability and mutagenesis [11, 12].
Instead, acute hypoxia is represented by a short-term hypoxia between a few minutes and up to 72h, which occurs when the vascular network in tumour tissue is defective. The process causes less tumour perfusion and, accordingly, hypoxia.
Moreover, the acute hypoxia could be promoted by temporal occlusion of blood vessels caused by blood clots or tumour emboli [13]. Acute hypoxia causes the production of high levels of reactive oxygen species (ROS) damaging cells.
In 2008, Bristow and Hill showed that hypoxia, changing the gene expression (Fig.2), favours the survival in a hostile environment.
Cancer cells to survive in hypoxic conditions adapt their metabolism reducing oxidative metabolism, activating autophagy [14, 15], increasing radio-resistance of cancer cells [16], promoting metastasis [17], and genomic instability [18].

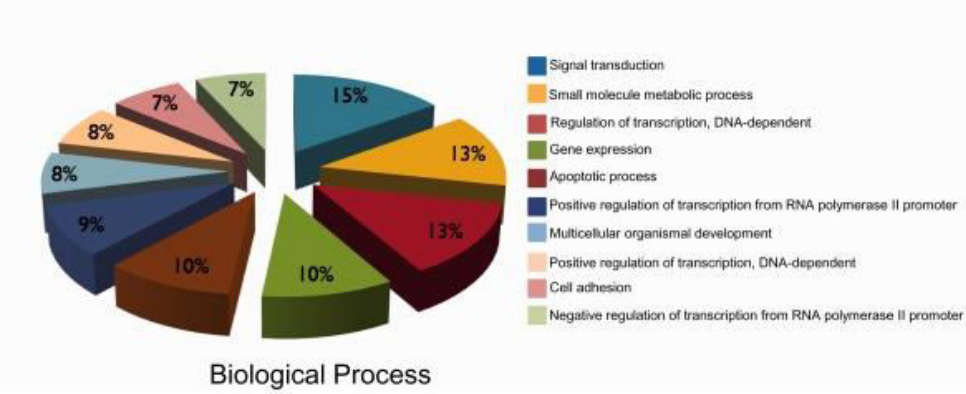

Fig.2: **Biological processes regulated by hypoxia.** (From Khurana P. et al. 2013)

1.2.1 Role of Hypoxia-Inducible Factor 1α (HIF-1α)

Hypoxia-Inducible Factor 1 (HIF-1) is a heterodimeric transcription factor consisting of an inducible subunit (HIF-1α) and a constitutively expressed subunit (HIF-1b) [19].
The heterodimer HIF-1 becomes active only in low oxygen conditions when HIF-1α subunit is stabilized. In fact, in normoxic conditions, HIF-1α is hydroxylated by a protein with an oxygen-dependent prolyl-4-hydroxylase domain (PHD), and then polyubiquitinated and degraded by the 26S proteasome [20].
The hydroxylation of HIF-1α form, followed by binding to a protein involved in its own ubiquitination and degradation called Von Hippel–Lindau (pVHL), promotes its degradation.
On the contrary, in low oxygen conditions the binding between pVHL and HIF-1α is inhibited, thus HIF-1α is stabilized, causing its accumulation and translocation into the nucleus.
In the nucleus, HIF-1α can bind to HIF-1b subunit forming the HIF-1 transcription factor.
HIF-1 recognizes and binds to the A/GCGTG consensus motif on the promoters of target genes, called hypoxia-responsive elements (HREs) [21].
Target genes are involved in different cellular pathways, such as glycolysis and pyruvate metabolism (GLUT-1, GLUT-3), angiogenesis (VEGF), cell proliferation (IGF2, TGF-a), pH regulation (CA-IX) and cell adhesion (MMPs) [22, 28] (Fig.3).
Accordingly, HIF-1 promotes cell survival, tumour neovascularization, cell migration, invasion through matrix-degrading enzymes and inhibits pro-apoptotic pathways. [29-30].
These effects cause chemotherapy and radiation resistance of tumour cells.

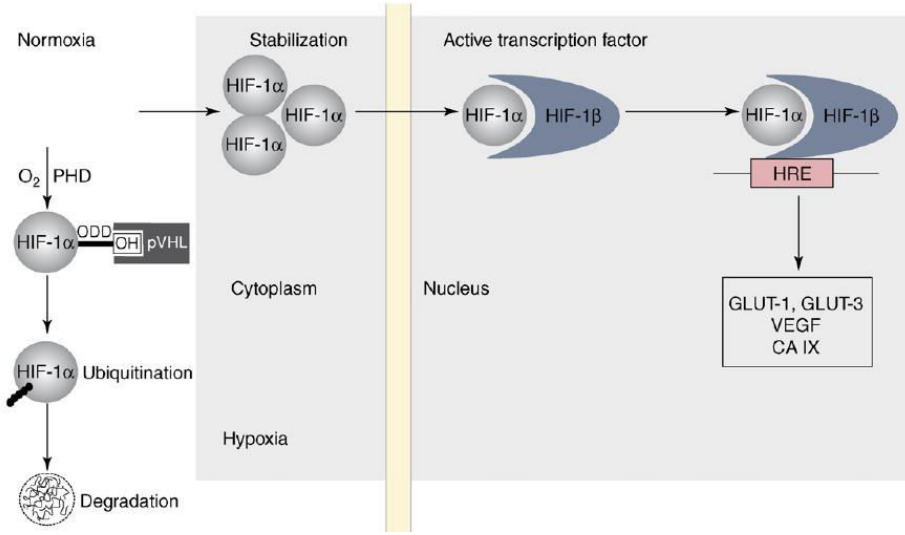

Fig.3: The role of HIF-1 during hypoxia. (From Thiry A et al. 2006)

1.3 Carbonic Anhydrases (CAs): role and function

Carbonic anhydrases (CAs) were discovered in 1933.
They are metalloenzymes grouped in five classes (α, β, γ, δ, ζ) basing on amino acid sequence, three-dimensional structure and their expression among different species [31-33].
The α-CA family was found in vertebrates; the β-CA family is in higher plants and some prokaryotes; γ-CA family is only in archaebacterial; δ-CA and ζ-CA classes are only in diatoms.
The CAs control intra- and extra-cellular concentrations of CO_2, H_2O, HCO^-_3 catalysing the conversion of CO_2 to the bicarbonate and protons: ($CO_2 + H_2O \leftrightarrow HCO^-_3 + H^+$).
Zinc ion (Zn^{2+}) in the active site is essential for the enzymatic activity.
The most characterized class is the α-CA because it is the unique expressed in mammals.
So far, 16 α-CA isoforms were found [34-36], differing in tissue distribution, subcellular localization and molecular properties (Fig. 4). Four evolutionarily unrelated gene families encode for all the isoforms found.
Three isoforms of the family do not present catalytic activity; they are known as CA-related proteins (CARPs): CARP VIII, CARP X and CARP XI.
Based on their subcellular localization, the α-CA family is divided in:

- cytosolic isoforms (CA I, CA II, CA III, CA VII, CA VIII, CA X, CA XI and CA XIII)
- glycosylphosphatidylinositol (GPI)-anchored isoforms (CA IV and CA XV)
- transmembrane isoforms (CA IX, CA XII, CA XIV)
- mitochondrial isoforms (CA VA and CA VB)
- secreted CA isozyme (CA VI)

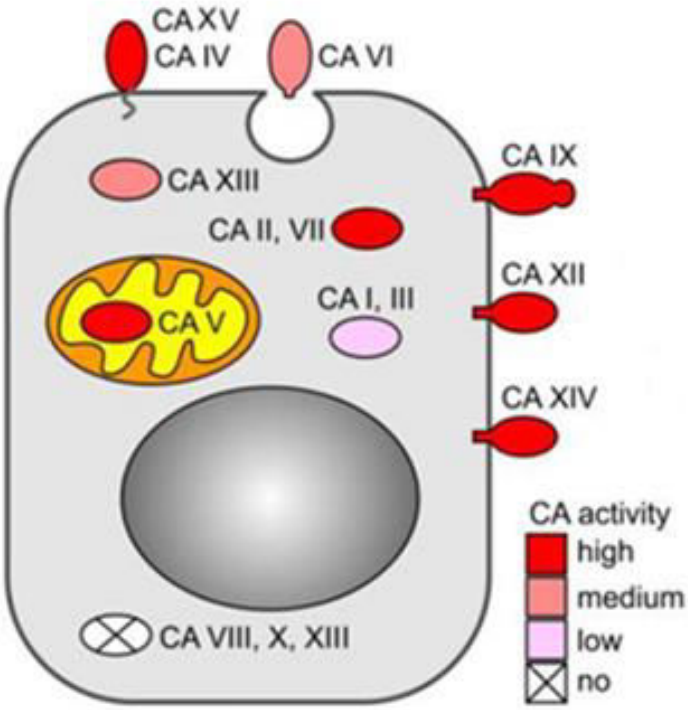

Fig.4: α-CA family: activity and subcellular localization. (Adapted from Zavada et al 1993)

Into the cells, the CAs control acid-base regulation, respiration, ion transport and bone resorption, electrolyte secretion, gluconeogenesis, lipogenesis and ureagenesis.
Among them, two transmembrane isoforms (CA-IX and CA-XII) are overexpressed in many types of solid tumours [37].

1.4 Carbonic Anhydrase IX (CA-IX)

1.4.1 Carbonic Anhydrase IX (CA-IX): gene location, structure and function

Pastoreková et al. detected CA-IX, at beginning called MN protein, in human cervix carcinoma HeLa cells in 1992 [38].
Two years later, Pastorekova et al. cloned the cDNA of the MN-protein and they observed that MN-protein showed a strong homology with the CA family, reason why it was called CA-IX.
CA-IX is located on chromosome 9p12-p13 [39] and it has a molecular weight of 49,7kDa.
CA-IX is a glycoprotein located on the cell surface; it exists primarily as dimer linked by disulphide bonds mediated by cysteine residues.
As shown in figure 5, CA-IX is composed by:

- N-terminal exofacial proteoglycan-like region (PG domain), which is adjacent to the catalytic domain. It is distinctive feature of CA-IX isoform;
- extracellular catalytic domain;
- transmembrane anchor;
- short C-terminal cytoplasmic tail.

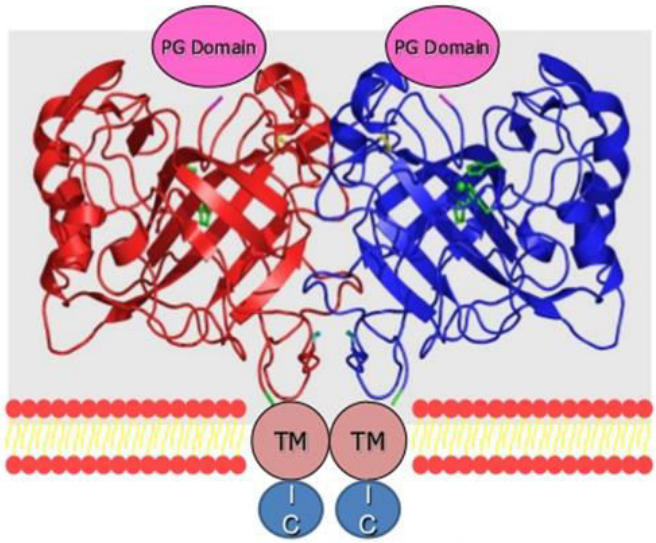

Fig.5: CA-IX structure: PG domain (a proteoglycan-like domain), the extracellular catalytic domain, TM (a transmembrane region) and IC (a cytoplasmic tail). (From Alterio V., et al. 2009)

1.4.2 The relationship between CA-IX and cancer

CA-IX and CA-XII are tumour-related isoforms, but CA-IX is interesting for its low expression in normal tissues.
CA-IX has the active site on the extracellular space and it efficiently catalyses the hydration of carbon dioxide to bicarbonate and protons reducing the extracellular pH (pHe).
As shown in figure 6, CA-IX acts on three interdependent points, called Jacob-Stewart cycle:

1. it produces extracellular protons, decreasing the pHe;
2. it supplies bicarbonate ions that, thanks to their transporter named bicarbonate transporters (BT), can cross the plasma membrane, consume cytoplasmic protons and neutralize intracellular pH (pHi);
3. it promotes CO_2 diffusion maintaining pHi>pHe gradient.

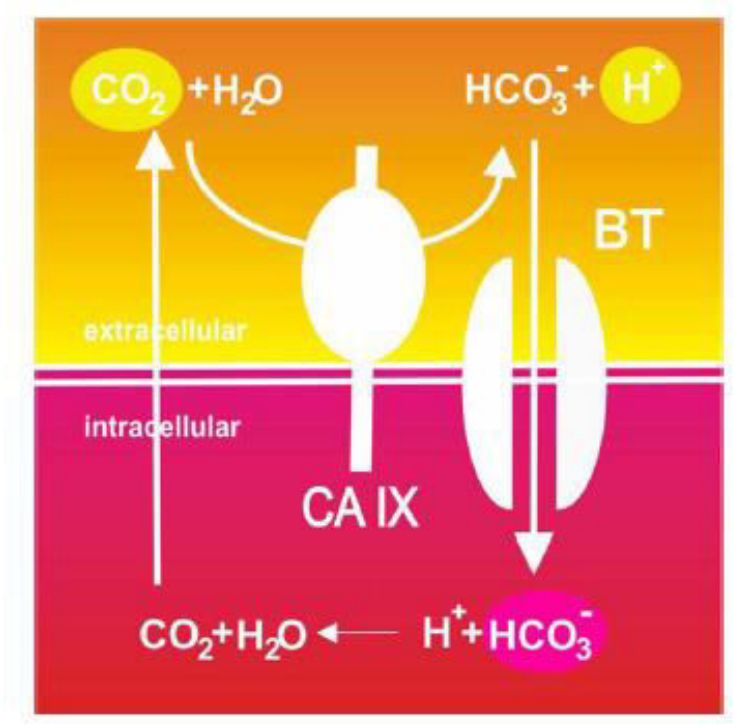

Fig. 6: Schematic illustration of the enzymatic role of CA-IX in pH regulation in tumour cells. (From Sedlakova O, et al. 2014)

CA-IX gene has HRE sequence localized immediately upstream the transcription initiation site. The HRE sequence permits a transcriptionally regulation by HIF-1 [40].
For this reason, the CA-IX expression is a hypoxic inducible enzyme.
Moreover, the CA-IX transcription is also increased by MAPK and PI3K pathways and tyrosine kinases, EGFR (epidermal growth factor receptor) and RET (Rearranged during Transfection) [41-43].
CA-IX expression is low or absent in normal tissues (except the intestinal and stomach mucosa, gallbladder and testis), but it is highly overexpressed in many types of cancer (Fig.7).
For example, CA-IX is overexpressed in clear-cell renal cell carcinoma caused by a mutation in Von Hippel– Lindau tumour suppressor, but not in normal kidney tissue. [44].
Furthermore, CA-IX is co-expressed in some tumour tissues together with oncogenic markers, such as LDH5, GLUT1, MCT4 [45-48].
Moreover, CA-IX overexpression confers resistance to chemotherapy, radiotherapy, and anti-angiogenic treatment. Preclinical evidences showed that tumours with high CA-IX levels are resistant to therapy, but its inhibition significantly improves chemo- or radio sensitivity [49-50].
Similarly, the CA-IX inhibition improves the anti-angiogenic therapy with anti-VEGF antibody [51]
Finally, CA-IX seems to have a role in cell-cell and cell-matrix interactions, cellular proliferation and migration [52-54].
For these reasons, CA-IX could be a good candidate for new diagnostic and therapeutic approaches.

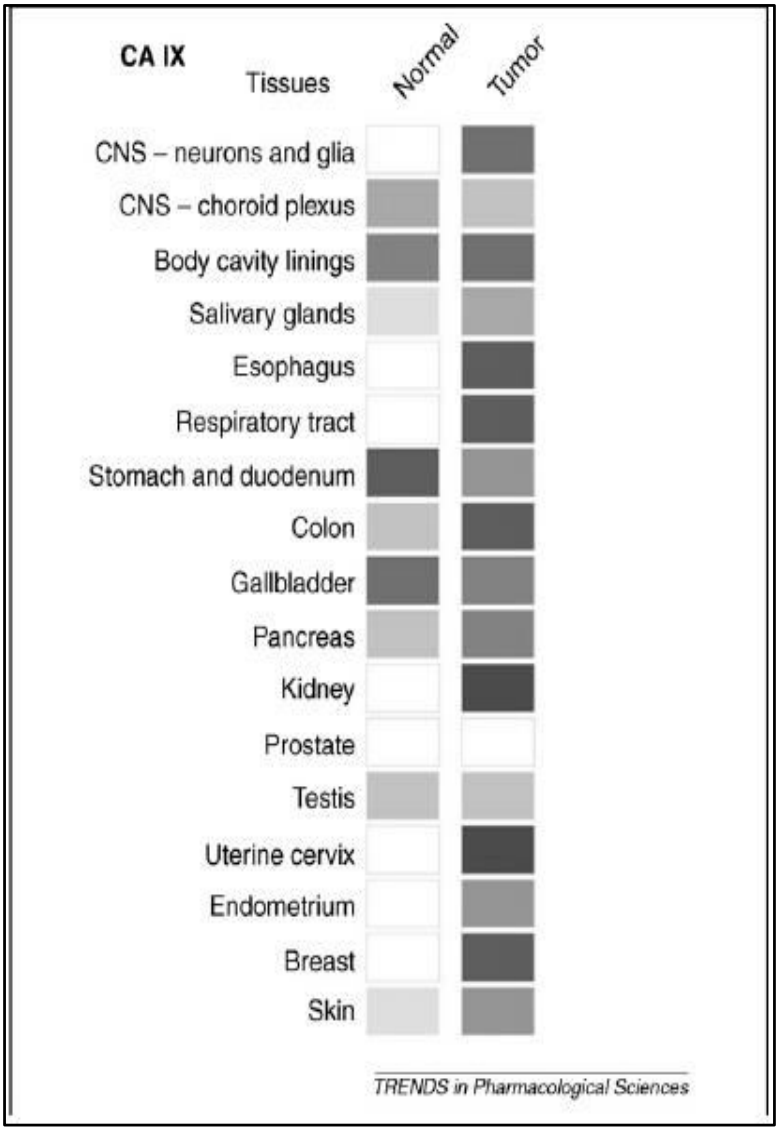

Fig. 7: CA-IX expression: normal tissues *versus* tumour tissues. (From Thiry A. et al 2006)

1.5 Aptamers

1.5.1 Composition and advantages of aptamers

Aptamers are short synthetic single stranded nucleic acids able to bind tightly to a target molecule [55].
The "aptamer" means "to fit" (aptus) in latin, that reflects two their important characteristics (Fig. 8):

- ability to fold into complex tertiary structures;
- ability to bind with high affinity and specificity to their targets.

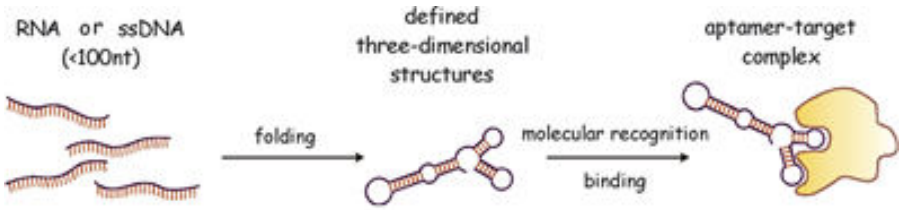

Fig. 8. Aptamers: Schematic representation of the aptamer functionality. (From Stoltenburg R. et al. 2007)

Aptamers act by directly binding to the protein target without interfering with its expression, unlike other small noncoding RNAs either natural or artificial, such as antisense, ribozymes, siRNAs and microRNAs (miRNA) that inhibit gene expression [56].
Aptamers are small nucleic acids of DNA or RNA, showing different characteristics.
The DNA aptamers are more stable due to the lack of 2′-OH groups.
However, there are numerous advantages of RNA aptamers.
Firstly, RNA aptamers make more structure thanks to strong intra strand RNA–RNA interactions [57].
Moreover, their stability can be enhanced using different types of modifications, such as the substitution of the 2'-ribose [58] with 2′-fluoro, 2'-amino pyrimidine (2'-F-Py, 2'-NH2-Py) or 2′-O-alkyl.
Modified RNA aptamers may survive, to degradation by nucleases, *in vivo* for several hours.
Thus, the RNA aptamers represent an attractive alternative as diagnostics and therapeutic tools compared to their peptide and monoclonal antibody counterparts [59-62] such as (Fig. 9):

1. easy chemical synthesis that results in a little or no batch-to-batch variation;
2. small size around 15-40kDa that allows a good penetration in tumour tissue;
3. low or no immunogenicity;
4. easy editing to improve their stability and half-life.

Furthermore, the oligonucleotides composition of the aptamers gives them a great stability at high temperatures compared to monoclonal antibodies and peptides that have limited shelf life, undergoing to denaturation at high temperature.

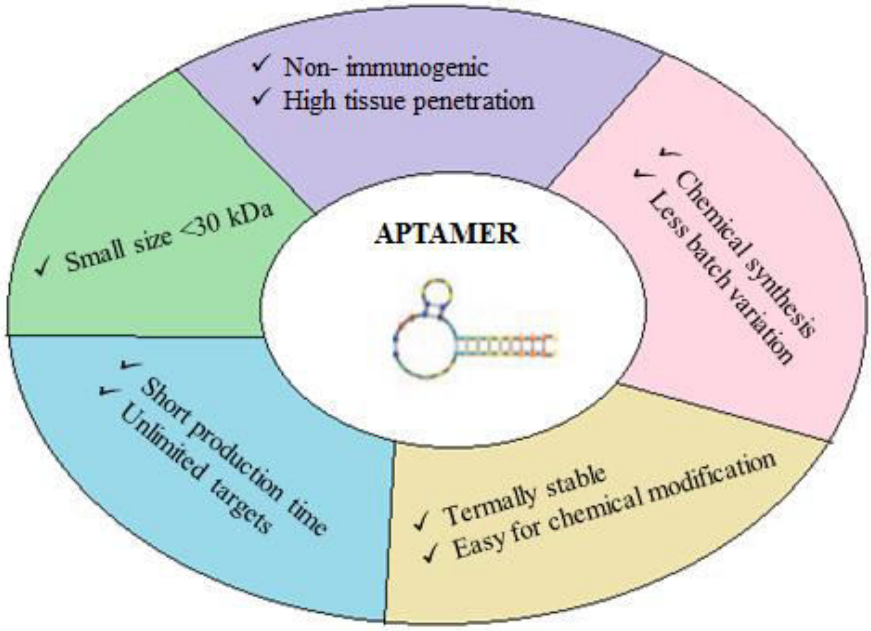

Fig. 9. : Advantages of aptamers.

1.5.2 Aptamer production: SELEX technology

The SELEX technology was developed in 1990. It is an evolutionary *in vitro* combinatorial chemistry process used to identify aptamers as specific ligands of a given target from large pools of different oligonucleotides [63].
The starting point for the generation of aptamers is the chemical synthesis of a single-stranded nucleic acid (RNA, DNA) library of large sequence complexity. A typical oligonucleotide library contains random sequences of 20–50 bases flanked by two constant regions that include primer sites for PCR amplification (Fig.10). Randomization is used to create possible sequences of enormous diversity (i.e. with n nucleotides in randomized region, 4^n different molecules), which generates a vast array of different conformations with different binding properties. As schematized in figure 10, the SELEX method includes several steps: (i) incubation of the library with the target molecule under favourable binding conditions; (ii) partitioning of molecules that, under the employed conditions, adopt conformations that permit binding to a specific target from other sequences; (iii) dissociation of the nucleic acid-protein complexes and (iv) amplification of the nucleic acids pool. The pool obtained from the first cycle will be then the starting pool for the next rounds of selection, thus reiterating these steps the library enriched in sequences that bind to the target is generated. After the final round, the resulting pool is subjected to DNA sequencing. Sequences corresponding to the initially variable region of the library are screened for conserved regions and structural elements indicative of potential binding sites and, subsequently, tested for their ability to bind specifically to the target molecule.
SELEX technology usually requires different cycles of selection, around eight or more, in order to isolate aptamers with nanomolar affinity.
Particularly, if the SELEX technology is performed on a protein, the rounds could be lesser than the SELEX technology performed on cells or tissues.
Even if many aptamers are still selected by the traditional *in vitro* methodology, over the last few years considerable efforts have been focused on automating *in vitro* selection procedures [64], thereby accelerating aptamers discovery.

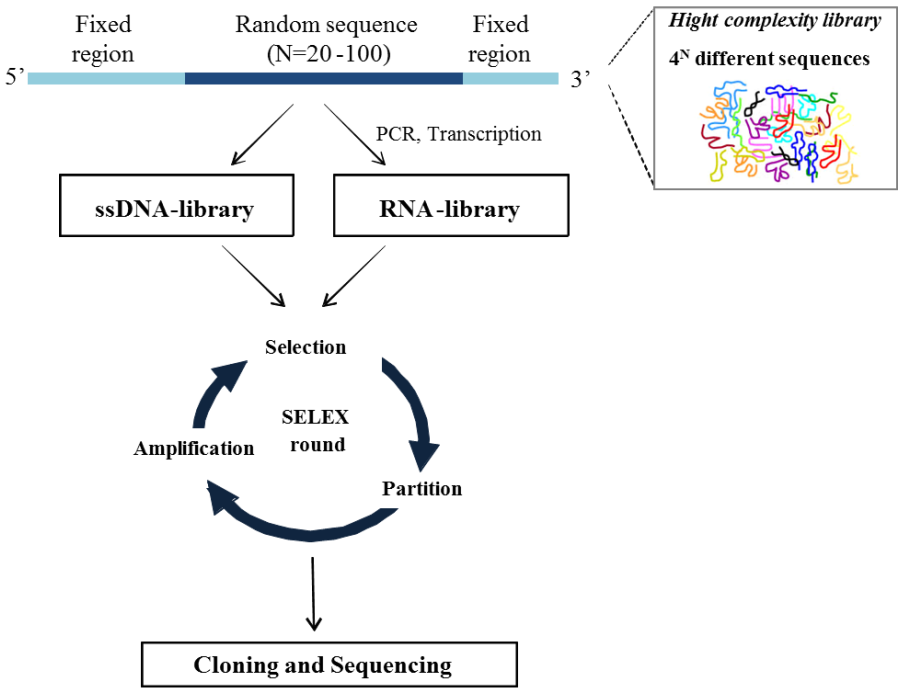

Fig. 10. Schematic representation of the SELEX technology. The RNA/DNA aptamers library contains a random sequence of 20–100 bases flanked by two constant regions. These constant regions include primer sites for PCR/RT-PCR amplification and transcription. The library is incubated with the target, not binding sequences are discarded whereas bound aptamers are recovered and amplified. (Adapted from Esposito C.L. et al 2011)

1.5.3 Cell-based SELEX

A great promise in developing specific molecular probes for disease biomarkers is recently represented by the intact cell-based SELEX strategy, that allows to select nucleic acid aptamers against living cells [65].
Aptamer selection approach that targets the cell surface open a new path which presents two major advantages: i) direct selection without prior purification of membrane-bound targets, ii) access to membrane proteins in their native conformation similar to the *in vivo* conditions. By using living cells as targets, aptamers able to discriminate cells from distant tumour types like small lung cancer cells *versus* large cell lung cancer [66], T-cell acute lymphocytic leukemia (ALL) *versus* B-cell lymphoma [67] and colon cancer cells *versus* other cancer cells [68] have been generated. Furthermore, by the SELEX technology against whole-living cells in culture [69] it was demonstrated that even by using complex targets as intact cells, it is possible to obtain aptamers against rare antigens if specifically expressed on the target cell.
In this regard, a panel of aptamers that bind a type of human malignant glioblastoma cells, discriminating them from non-tumorigenic glioblastoma cells, was isolated by a differential cell-SELEX approach [70]. In addition, the great advances in cell-SELEX offer also the opportunity to develop innovative approaches to identify and isolate cancer stem cells that are emerging as important target to develop more effective cancer therapy [71].
During the cell-SELEX strategy, to avoid the selection of ligands that recognize multiple surface proteins along with the target of interest, the counter- or negative-selection is critical.
A negative selection step using negative cells was included to enhance the specificity of the aptamers and prevent the enrichment of aptamers for abundant non-specific proteins.
Thus, for each cycle of the cell-SELEX strategy, the library is first incubated with non-target cells as counter-selection step (negative selection). Unbound aptamers are, then, recovered and incubated with the target cells. Bound aptamers are recovered and amplified (see Fig 11).
Moreover, to improve the affinity and specificity of the aptamers the selective pressure during the cell-SELEX protocol is increased changing several conditions:

1. The increase of the washes number after the incubation is important to eliminate weakly bound or unbound aptamers.
2. the reduction of the cells number is important to reduce the quantity of the target molecule in order to recover only the aptamers with the best affinity and discard the aptamers with the limited binding capability.
3. the increase of the counter-selection numbers instead is important to discard the most of aptamers recognizing non-specific target molecules.
4. the addition of polyanionic nucleic acid, as yeast tRNA, salmon spermidine or polyinosine, avoids binding depending only on the opposite charge between basic proteins and the negatively charged nucleic acids.

The cell-SELEX approach has been further developed to discriminate even different properties in the same cancer cell type (such as malignancy, therapeutic response, metastatic potential).
Moreover, to cell-SELEX, even a tumour implanted in mice (*in vivo*-SELEX) have been used to select aptamers [72].
Recently, more sophisticated approaches combine fluorescence activated cell sorting (FACS) technology with *in vitro* selection (FACS–SELEX) has been performed [73], thus enabling a live-cell/dead-cell separation within a cultured cell mixture.

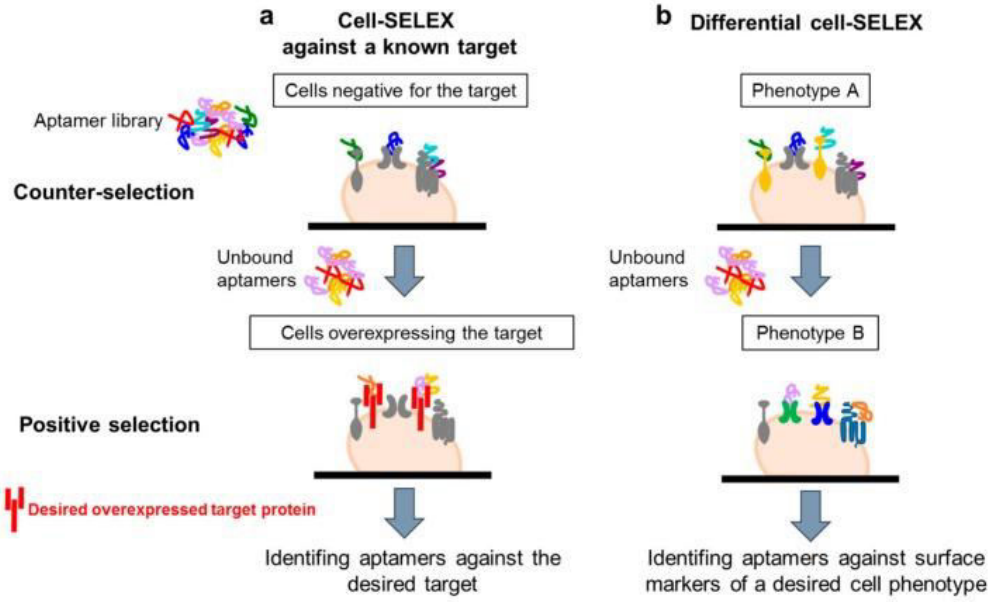

Fig. 11. Cell-based SELEX. **a)** A pool of RNAs is incubated with non-target cells (counter-selection). Unbound sequences in the supernatant were recovered, and incubated with cells overexpressing the target for the selection step (positive selection). Unbound sequences were discarded by washings and bound sequences were recovered by total RNA extraction. **b)** Cell-based SELEX protocol to identify multiple ligands specifically. recognizing a cell phenotype, without prior knowledge of the target protein. (Catuogno S. et al. 2017)

1.6 Aptamers in therapy and diagnosis

1.6.1 Modifications of aptamers for clinical applications

Aptamers usable for clinical applications are usually modified in order to optimize their pharmacokinetic (PK) and pharmacodynamic (PD) profiles (see Fig. 12).
Since aptamers, especially RNA-based aptamers, are rapidly degraded by nucleases in whole organisms, major efforts have been addressed to improve their stability by a variety of approaches [74].
The most typical modifications to enhance the stability of aptamers are the substitution of the 2'-ribose [17]. RNA aptamers with 2′-fluoro, 2'-amino pyrimidine (2'-F-Py, 2'-NH2-Py) or 2′-O-alkyl nucleotides modifications may survive for several hours *in vivo* against degradation by nucleases.
Another example of modified nucleic acids is represented by the Spiegelmers. They do not contain additional groups added to the sugar moieties, but are enantiomers of natural nucleic acids [75]. In particular, the natural D-nucleic acids are substituted with enantiomeric L-nucleic acids. This property prevents recognition by nucleases, increasing the stability.
A hurdle in administering of aptamers to patients for many therapeutic applications is a short circulating half-life due to their small size. While a low molecular weight can be an advantage because it allows economical chemical synthesis and better target accessibility, it promotes rapid clearance by the renal system. By simply increasing the molecular weight of the aptamers, the circulating half-life can be significantly extended.
The most common method to increase the aptamers size is to add a polyethylene glycol (PEG) moiety or cholesterol tail [76].

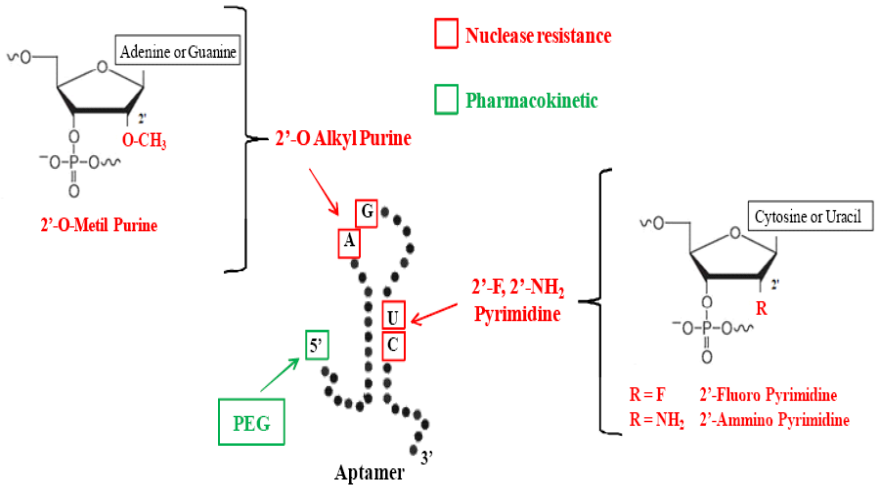

Fig. 12. Aptamer modifications. Scheme of the most typical modifications used to improve aptamer nuclease resistance (red) or its pharmacokinetic profile (green).

1.6.2 Aptamers as therapeutics

In the last years, the development of aptamers as therapeutics has primarily involved aptamers that bind and inhibit the activity of their protein targets.
The list of aptamers against important therapeutic targets is growing rapidly and a handful of aptamers is now in clinical trials as therapeutic agents (see Table 1).
To date, the most successful therapeutic application is represented by an RNA aptamer, named Macugen, binding and antagonizing the action of Vascular Endothelial Growth Factor (VEGF), a growth factor that promotes the blood vessel formation (vascularization) [77].
Macugen (or Pegaptanib, marketed by Pfizer) has been demonstrated in phase III clinical trials to be effective for diabetic retinopathy treatment.
The aptamer has been fully approved by the Food and Drug Administration (FDA) in December 2004 for the treatment of age-related macular degeneration (AMD). It is characterized by the formation of a neovascular membrane leaking blood and fluid under the retina with consequent destruction of the macula and loss of vision [78]. The aptamer binds and antagonizes the action of VEGF-165, the VEGF isoform preferentially involved in pathological ocular neovascularization. With the intent to improve the pharmacodynamic and pharmacokinetic properties of this 28-mer aptamer, it was chemically modified with 2′-F-Py and 2′-OMe-Pu, capping, and linkage to a 40kDa branched PEG molecule, which increases the intravitreal residence time of the molecule.
Different studies have been carried out to assess the clinical cost-effectiveness of Macugen comparing to Ranibizumab (Lucentis, Genentech), a monoclonal antibody targeting all isoforms of human VEGF-A, approved in 2006 by the FDA for the treatment of exudative AMD.
Both drugs show comparable therapeutic efficacy and mild adverse events, while the economic evaluation varies considerably depending on the methodology for cost-effectiveness used in different studies.
Many other aptamers, not yet approved by the FDA, are currently in clinical trials.
Among them, it is very interesting for cancer therapy the AS1411 DNA aptamer (AGRO100) directed against nucleolin [79], a protein often overexpressed on the surface of cancer cells. This DNA aptamer is part of the guanine-rich oligonucleotide class of aptamers that form G-quartets, a structural element that exhibits a proliferative activity.

Once bound to nucleolin, the AS1411 aptamer is taken into the cancer cell, where it causes cellular death by apoptosis through inhibition nuclear factor-κB (NF-κB) [80] and Bcl-2 [81] pathways.
It showed its effectiveness as an anticancer therapy for different solid human malignancies as well as for acute myeloid leukemia (AML) and it is currently in phase IIb clinical trial to evaluate its effectiveness in combination with high-dose of cytarabine in patients with relapsed and refractory AML.

Name	Form	Target	Condition	Phase
Pegaptanib sodium (Macugen)	27-nt RNA	VEGF (Vascular Endothelial Growth Factor)	Age-related macular degeneration	Approved
E10030	29-nt DNA	PDGF (Platelet-Derived Growth Factor)	Age-related macular degeneration	Phase III
REG1 (RB006 and RB007)	37-nt RNA	Coagulation factor IXa	Coronary artery disease	Phase III
ARC1905	38-nt RNA	C5 (Complement component 5)	Age-related macular degeneration	Phase III
AS1411	26-nt DNA	Nucleolin	Acute myeloid leukemia	Phase II
ARC1779	39-nt DNA	A1 domain of von Willebrand factor	Von Willebrand disease/thrombotic thrombocytopenic/purpura	Phase II
NOX-E36	40-nt RNA	CCL2 (Chemokine C-C motif Ligand 2)	Chronic inflammatory diseases/type 2 diabetes mellitus/systemic lupus erythematous	Phase II
NOX-A12	45-nt RNA	CXCL12 (Chemokine C-X-C motif Ligand 12)	Multiple myeloma and non-Hodgkin lymphoma/autologous or hematopoietic stem cell transplantation	Phase II
NU172	26-nt DNA	Thrombin	Heart disease	Phase II
NOX-H94	44-nt RNA	Hepcidin peptide hormone	Anemia/end-stage renal disease/inflammation	Phase II
ARC19499	32-nt RNA	TFPI (Tissue Factor Pathway Inhibitor)	Hemophilia	Phase I

Table 1. Aptamers in on-going or completed clinical trials. (From Zhenjian Z. et al. 2017)

1.6.3 Aptamers as delivery agents

The aptamers can be also internalized together with their target receptor. For this reason, they can be used to deliver any kind of secondary reagents to a given cancer cell or tissue (Fig. 13).

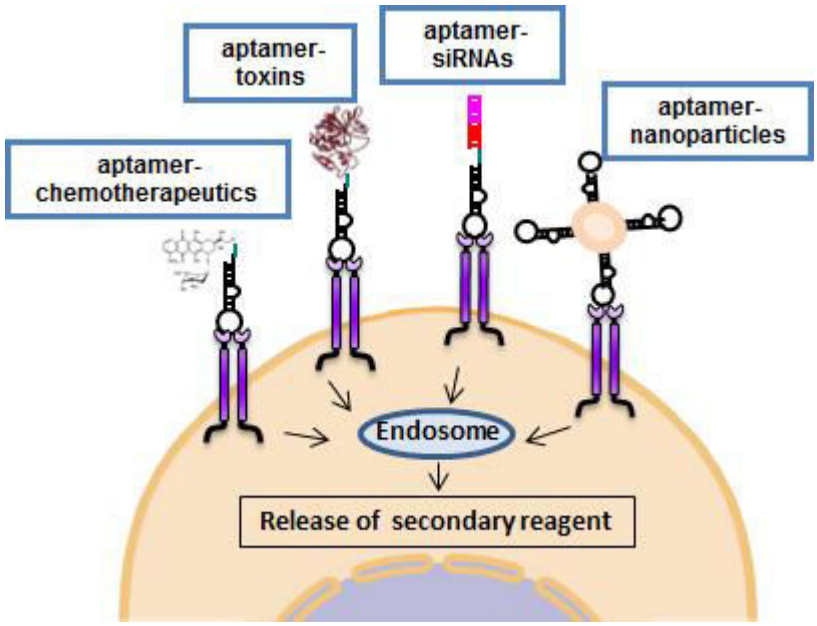

Fig. 13. Aptamers as delivery agents. Aptamers that bind to cell surface receptors can be used to deliver small interfering RNAs (siRNAs and miRNAs), toxins, radioisotopes, and chemotherapeutic agents to target cells. (From Catuogno S. 2013)

In this way, only targeted cells will be exposed to the secondary reagent, thus increasing the efficacy of a given therapy as well as attenuating the overall toxicity of the drug [82]. In this regard, currently an increasing number of aptamers targeting cancer cell surface epitopes have been successfully used for the specific delivery of active drug substances both *in vitro* and *in vivo*, including nanoparticles, anti-cancer therapeutics, small interfering RNAs (siRNAs), microRNAs, toxins [83], enzymes [84], radionuclides [85], viruses [86].
Several cell-internalizing aptamers against surface epitopes of cancer cells have been successfully used as targeting vehicles. These include aptamers against the protein tyrosine kinase 7 (PTK7), nucleolin, prostate specific membrane antigen (PSMA), mucin 1 (MUC1) and EGFRwhich have been selected through either protein- or cell-SELEX strategies [87].

To date, the best characterized for targeted delivery are the 2'F-Py-RNA aptamers against the extracellular domain of PSMA (A9 and A10). These aptamers have been used to deliver nanoparticles, quantum dots, toxin or siRNA to prostate cancer cells. PSMA–aptamers has been linked to siRNAs by different approaches including non-covalent conjugation (Fig. 14), via a streptavidin connector, or generation of aptamer–siRNA chimeras, by extending the 3'end of the aptamer with a nucleotide sequence complementary to the antisense strand of the siRNA. In addition to siRNAs, PSMA–aptamers has been further used to deliver to prostate cancer cells toxins or chemotherapeutic agents encapsulated within nanoparticles or directly intercalated into the nucleic acid sequence [88].
Another promising delivery molecule is the phototoxic aptamer against MUC1 that carries the toxin chlorin *e*6, a heme-like photodynamic therapy (PDT) agent released after activation by light. MUC1 is a membrane specific marker expressed on a broad range of epithelial cancer cells such as breast, ovary, prostate, pancreas, colon and lung. After the binding of the aptamer, the new complex is internalized and routed through endosomal and Golgi compartments by cancer cells. The aptamer directed at the MUC1 peptide is armed to carry a cytotoxic cargo such as the light-activated PDT drug, chlorin *e*6, that produce cytotoxic singlet oxygen species. After light activation,the complex ability to kill epithelial cells was enhanced by several orders of magnitude in comparison to free drug alone. As a result, there is a selective induction of apoptosis in MUC1 expressing cells [89].
In addition, John Rossi's group used a RNA aptamer against gp120 for targeted delivery of siRNA against Human Immunodeficiency Virus (HIV) infections [90].
So far, the number of aptamer-siRNA conjugates described in literature has rapidly expanded providing new promising therapeutic options [91].
Furthermore, recent few papers explored the use of aptamer to deliver microRNAs as cancer therapeutics.
Second generation PSMA targeting aptamer (A10-3.2) was conjugated to polyamidoamine (PAMAM)-based microRNAs (miR-15a and miR-16-1) via bifunctional PEG to deliver microRNAs to prostate cancer cells. In addition, chimeras that combines MUC1 aptamer and let-7i microRNA or miR-29b have been reported. These new compounds provide innovative cancer therapeutic strategies even if their *in vivo* effectiveness has not been proven. Recently, Esposito et al. demonstrated the in vivo effectiveness of an aptamer-miRNA conjugate for lung cancer targeting. The authors designed a dual-function molecules containing an RNA

aptamer (GL21.T), directed against the RTK Axl, covalently linked to miRNA let-7g [92]. The same aptamer was also used for the delivery of miR-212 to restore TRAIL-mediated cytotoxicity in NSCLC cells [93]. On the other end, Catuogno et al. described for the first time an aptamer-based system for the delivery of therapeutic single strand antimiRs [94]. Furthermore, very recently miRNA and antimiR delivery has been integrated developing a novel combined therapeutic approach for glioblastoma stem-like cells (GSCs) therapeutic targeting [95].
Moreover, the non-covalently link of the drugs to the aptamers was studied in order to understand if there is an abolishment of the aptamer binding and if the drug is released from the aptamer.
This model was studied with doxorubicin (DOX) intercalated with the aptamers against PSMA for prostate cancer [96], MUC1 [97].
This doxorubicin approach has shown toxicity levels compared to the free doxorubicin, but only in the cancer cells, reducing general toxicity or cardiotoxicity thanks to the specific aptamer delivery.

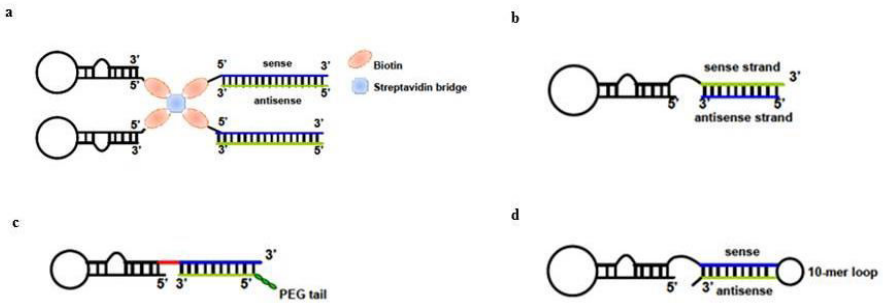

Fig. 14. Anti-PSMA aptamer-siRNA chimeras. (a) The RNA duplex and RNA aptamers are chemically conjugated with biotin. Thus, two biotinylated siRNAs and two aptamers are non-covalently assembled via streptavidin; (b) The 3′ end of the aptamer is extended to contain the nucleotide sequence that is complementary to the antisense strand of the siRNA, and the chimera is formed by annealing the aptamer to the siRNA antisense strand; (c) optimized chimeras in which the aptamer portion of the chimera is truncated, and the sense and antisense strands of the siRNA portion are swapped. A two-nucleotide 3′-overhang and a PEG tail are added to the chimera; (d) the 3′-terminus of the aptamer is conjugated to the sense strand of the siRNA, followed by a 10-mer loop sequence and then by the antisense strand of the siRNA. (From Cerchia L. et al. 2011)

1.6.4 Aptamers in cancer imaging, diagnosis and biomarker discovery.

In the early stage of tumorigenesis, the cancer cells number is very low and for this reason, the detection is an important challenge.
Thus, to find new methods high sensitive to detect the cancer cells are very important.
Thanks to their characteristics, aptamers have also started to play increasingly important roles in the human disease diagnosis [98].
Indeed, since the chemistry for the production and modification of oligonucleotides is well developed, once aptamers are selected, they can be functionalized using a wide variety of fluorophores, as well as conjugated with superparamagnetic iron oxide nanoparticles, Mn_3O_4- or gold nanoparticles, radioisotopes and biotin. These characteristics make the aptamers suitable as ligands for protein detection in a great number of different methodologies.
Due to their relatively small size (8-15kDa) in comparison to antibodies (150kDa), aptamers should be better suited for a rapid tumour penetration and blood clearance, two excellent characteristics for imaging and diagnosis technologies. Hicke et al. were the first that published the use of a radiolabelled aptamer, named TTA1, for *in vivo* tumour target imaging [99].
TTA1 is a modified RNA aptamer against tenascin-C, an extracellular matrix protein upregulated in a number of tumours such as breast, lung, colon, prostate, glioblastoma, and lymphoma [100]. The aptamer was conjugated to the Technetium-99m (99mTc) and it was intravenously injected in mice bearing glioblastoma (U251) and breast (MDA-MB-435) tumour xerographs [99], with the purpose of performing single photon emission-computed tomography (SPECT), a 3D-imaging technique that can aid in visualizing tumours.
The authors obtained a good tissue penetration and an important ratio tumour-to-blood of TTA1 aptamer.
This study suggests a quickly blood clearance and long tumour retention.
As shown in table 2, many other DNA or RNA aptamers have been developed for diagnosis of human diseases.
Moreover, aptamers are useful in many imaging techniques such fluorescence and bioluminescence imaging, magnetic resonance imaging (MRI), positron emission tomography (PET), single photon emission tomography (SPECT), computed tomography (CT) and ultrasound (US) [101,102].

Name	Target	K_d (nM)	Sensitivity	Specificity
		Cancers		
XL-33	Metastatic colon cancer cells (SW620)	0.7	81.7% (n = 71 metastatic colon cancer tissues)	66.7% (n = 18 non-metastatic colon cancer tissues)
yl19	Cholangiocarcinoma cells (QBC-939)	42.4	-	100% (n = 6 cancer cell lines)
LXL-1	Metastatic breast cancer cells (MDA-MB-231)	44.0	76% (n = 34)	100% (n = 8 cancer cell lines)
SYL3-C	Solid cancer Epithelial Cell Adhesion Molecule (EpCAM)	22.8	60%	100% (n = 3)
GMT3	Glioblastoma multiforme cells (A172)	75.3	-	87.5% (n = 8 cancer cell lines)
		Cardiovascular Diseases		
Myo040-7-27	Myoglobin	4.93	10 pm	-
		Infectious Diseases		
LmWC-25R and LmHSP-7b/11R	Leishmania promastigote and hydrophilic surface protein	-	100 ng (parasite protein)	-
2008s	*Plasmodium falciparum* lactate dehydrogenase	42–59	57 ng/mL	No human LDH recognition

Table 2. Recently developed aptamers for the diagnosis of human diseases. (From Zhuo Z. et al. 2017)

Until now, the aptamers are used for *in vitro* purpose such as dot-blot [103], western blot applications [104, 105], in the sandwich assay called ELONA (Enzyme Linked Oligonucleotide Assay).

In addition to their role as imaging tools, aptamers can also aid in clinical *in vitro* diagnosis of diseases and discovery of new biomarkers.

Recently, several groups developed aptamer-based biomarker discovery platforms.

For example, Gold co-workers described an aptamer chip for the biomarker discovery. The system is able to measure thousands of proteins together from serum or plasma samples [106].

Novel aptamer-based technologies will continue to evolve and they could provide enormous opportunities in different diagnostic area.

2. AIM OF THE STUDY

Hypoxia is a hallmark of many types of solid tumours.
It is associated with an aggressive tumour phenotype and therapeutic resistance.
During the hypoxia, the transcription factor HIF-1 binds to HRE present in its target genes, such as CA-IX, resulting overexpressed.
CA-IX expression promotes the acidification of the microenvironment that might decrease the uptake of weakly basic anticancer drugs, leading to chemo resistance.
For this reason, an accurate detection and inhibition of CA-IX could represent an important approach to improve the conventional therapies and the early diagnosis of the cancer.
Aim of the present study is to find new tools aptamer-based able to bind CA-IX.
In order to identify a panel of RNA aptamers which bind to CA-IX, two cell-SELEX protocols were designed (called Physiological cell-SELEX and Specific cell-SELEX**).**
Following screening and matching of two pools, the selected aptamers and its truncated sequences further investigated for specificity, serum stability and albumin binding.

3. MATERIALS AND METHODS

3.1 Cell culture

Cell lines were purchased from the ATCC (LG Standards, Milan, Italy). COS7, MDA-MB-231 and U87MG cells were grown in Dulbecco's modified Eagle's medium (DMEM) supplemented with 10% heat-inactivated fetal bovine serum (FBS) and 100 U/ml penicillin/streptomycin. All cell culture reagents were purchased from Sigma (St Louis, MO).

3.2 Hypoxia induction

Physical method: $2x10^5$ U87MG cells were seeded in p35 cell plate in serum-free medium, and put in the hypoxic incubation chamber maintained at 5% O_2. The cells were recovered at different times (6, 24, 48h).
Chemical methods: $2x10^5$ U87MG or MDA-MB-231 cells were seeded in p35 cell plate. U87MG or MDA-MB-231 cells were incubated with 100-150-200μM of Cobalt (II) Chloride hexahydrate (Sigma, St Louis, MO) dissolved in the serum-free medium and put in a conventional incubator (37°C; 5% C02). At different times (1, 6, 24h) the cells were recovered.

3.3 CA-IX cDNA transfection and acidic condition

Human CA-IX ORF clone (NM_001216) (Origene, Rockville, USA) was transfected with Lipofectamine 2000 (Invitrogen, Waltham, MA, USA), according to the manufacturer's protocol.
For the acid condition, the MES buffer (morpholinoethanesulfonic acid) (Sigma, St Louis, MO) was added to the serum-free DMEM from 45 to 90mM for different incubation times (30, 90, 180 minutes). The pH medium was measured by a pHmeter (Mettler Toledo, Columbus, Ohio,USA).

3.4 Immunoblotting

Cells were washed twice in ice-cold phosphate-buffered saline (PBS) (Sigma St Louis, MO), and lysed in the JS buffer containing:

- 50 mM Tris-HCl pH 7.5
- 150 mM NaCl
- 1% Nonidet P-40
- 2 mg/ml aprotinin
- 1 mg/ml pepstatin
- 2 mg/ml leupeptin
- 10 mM Na3VO4

Protein concentration was determined by Bradford assay (Biorad, Hercules, CA, USA).
The cell lysates were denatured in Laemmli buffer (2% SDS , 5% β-mercaptoethanol, 0,001% Bromophenol Blue, 10 % glycerol) for 5 minutes at 100°C, and then subjected to SDS-PAGE.
12% Acrylamide/bis-acrylamide gels were electroblotted into polyvinylidene difluoride (PVDF) membranes (Millipore Co., Bedford, MA, USA)
Filters were probed with primary antibodies as indicated.
The primary antibodies used are: anti-CA-IX (R&D Systems, Minneapolis, MN. USA); anti-HIF-1α (BD Biosciences, Qume Drive San Jose, USA); anti-α-tubulin (Santa Cruz Biotechnology, CA, USA); anti-vinculin (Cell Signaling Technology, Danvers, MA); anti-β-actin (Santa Cruz Biotechnology, CA, USA). Donkey anti-goat, goat anti-mouse and goat anti-rabbit (Santa Cruz Biotechnology, CA, USA) were used as secondary antibodies.

3.5 Immunofluorescence

To assess CA-IX expression on the cell surface, MDA-MB-231 cells in normoxic condition or stimulated with $CoCl_2$ (150μM) for 24h to mimic hypoxic condition, were seeded on poly-l-Lysine coated glass coverslips and incubated with anti-CA-IX antibody for 30 min at 37 °C prior to fixation. Cells were, then, fixed with paraformaldehyde 4% in PBS for 10 minutes and incubated at 37°C for 30 minutes with Alexa568 secondary antibody (Invitrogen, Waltham, MA, USA). Coverslips were then mounted on microscope slides with Prolong Gold Antifade Reagent with DAPI (Invitrogen, Waltham, MA, USA) and visualized by confocal

microscopy. Images were obtained using a Zeiss 510 LSM confocal microscope with a 40 × oil objective.

3.6 Physiological cell-SELEX

The SELEX cycle was performed essentially as described (Fitzwater and Polisky 1996). Transcription was performed in the presence of 1mM 2'-F pyrimidines and mutant T7 RNA polymerase (2.5u/ml T7 R&DNA polymerase, Epicentre Biotechnologies, Madison, Wisconsin) to improve yields.
2'F-Py RNAs were used to increase the resistance of the aptamers to degradation by sieric nucleases. 2'F-Py RNAs were heated at 85°C for 5 min, snap-cooled on ice for 2 min, and allowed to warm up to 37°C.
The Hypoxic cell-SELEX protocol is composed by twelve cycles.
Counter-selection step against normoxic MDA-MB-231 cells.
To avoid the selection of aptamers recognizing normoxic targets on MDA-MB-231 surface, the pool was firstly incubated on normoxic MDA-MB-231 for 30 min (up to round 6) or for 15 min (for the following rounds) at 37°C.
In each cycle the SELEX conditions were changed such as the dimension of the cell culture dishes (150mm, 100mm, 50mm, 35mm). Unbound sequences were recovered for the selection step.

Selection step against hypoxic MDA-MB-231cells.
The recovered sequences were incubated on $CoCl_2$-stimulated MDA-MB-231 cells (to mimic the hypoxic condition).
After several washings, sequences were recovered by total RNA extraction.
During the selection process, the selective pressure was changed increasing washings number (from one for the first cycle up to five for the last cycles), decreasing the incubation time (from 30 to 15 min from round 7) and the dimension of the cell culture dishes (150mm, 100mm, 50mm, 35mm). It was also increased the number of counter-selection steps from one to two from round 8.
Moreover, the use of a non-specific competitor, named yeast tRNA (Sigma, St Louis, MO), was introduced at different concentrations: 100μg/ml for the round 10 and 200μg/ml for the round 11; in the last two cycles (11 and 12) the pre-treatment with yeast tRNA before of the 2'F-Py RNAs pool incubation was made.

3.7 Specific cell-SELEX

The starting pool is represented by the 9th cycle of Physiological cell-SELEX.
The counter-selection step was performed against COS7 wild type (COS7-WT) cells to avoid the selection of aptamers that recognize proteins normally expressed on COS7 cells.
The selection step was performed against transient transfected COS7 with the CA-IX cDNA (called COS7-CAIX) in order to select specific aptamers for the target.
For each cycle, the pool of 2'F-Py RNAs was firstly incubated on the COS7 wild type cells at 37°C, the 2'F-Py RNAs that not bind these cells are recovered and incubated on CA-IX-COS7 for the selection step.
After several washes, the sequences were recovered by total RNA extraction.
During the SELEX process, the selective pressure was progressively enhanced increasing washings number (from five for the round 10a up to six for the rounds 11a and 12a), increasing the number of counter-selection steps from two in 10a and 11a cycles to three for the last cycle (12a). The yeast tRNA 100µg/ml as a nonspecific competitor (Sigma, St Louis, MO) was used in 10a and 11a cycles; in the last two cycles (11aand 12a) it was also added the pre-treatment with yeast tRNA.
Each cycle was checked for CA-IX expression.

3.8 RT-PCR, mutagenic and non-mutagenic PCR for cell-SELEX method

The RNA extracted from each SELEX cycle was retro-transcribed using Tetro Reverse Transcriptase Enzyme (Bioline, London, UK) according to the manufacturer's protocol. The retro-transcription reaction was as follow: 90°C for 3min, 42°C for 15min and 50°C for 30min.
The product was used for mutagenic PCR, characterized by higher concentration of $MgCl_2$ (6mM) and dNTP 1mM, using 0.5U/µl of FIREpol DNA Polymerase (Microtech, Milan, Italy) and 0,3µM primers:
N40 (Forward):5'-TTCAGGTAATACGACTCACTATAGGGAAGAGA AGGACATATGAT-3'
N40 (Reverse): 5'-TCAAGTGGTCATGTACTAGTCAA -3'
The reaction was as follow: 95°C for 5min, 10 cycles of 95°C for 1 min, 65°C for 1min and 72°C for 1 min, and a final extension of 72°C for 1min.

The last SELEX cycle is amplified by non-mutagenic PCR using 0.1U/µl of FIREpol DNA Polymerase and 200µM dNTP, not adding MgCl2 to that contained in the Taq Buffer.
The reaction was as follow: 95°C for 5min, 8 cycles of 95°C for 30 sec, 65°C for 1min and 72°C for 1 min, and a final extension of 72°C for 5min.
Amplified DNA was purified using Amicon Ultra Centrifugal Filters (Millipore, Massachusetts, USA).
At the end of SELEX method, sequences of the pools were subjected to cloning with TOPO-TA cloning kit (Invitrogen, Waltham, MA, USA).
The sequences have been analysed for multiple alignment (ClustalW by EMBL-EBI) and structural elements (MFOLD by unafold) indicative of potential binding sites.

3.9 Cell binding assay by RT-qPCR

The binding assay of individual aptamers was performed in 6-well plates in triplicate on COS7-CA-IX cells as positive cells and COS7-WT as negative cells. 10^5 cells per well were seeded and, 24 hours after transfection, were incubated for 30 minutes with serum-free medium in presence of yeast tRNA 200µg/µl and MES buffer (60mM). Then, 100nM of aptamers were added for 15 min at 37°C. Following three washes with PBS to remove unbound aptamers, the bound sequences were recovered by TRIzol (Life Technologies, Carlsbad, CA, USA) containing 0.5pmol/ml of reference control. The amount of bound RNAs was determined by RT-qPCR.
At each experiment, cells cultured were counted. The obtained data were normalized to the reference control and to cell number.

3.10 *In vitro* human serum stability

2'-F-RNA S-47s1 and S-51s1 aptamers were incubated at 4µmol/l concentration in 87% human serum (Type AB Human Serum provided by Euroclone, Milan, Italy) from 1 to 72 hours at 37°C.
At each time point 2µl (8 pmoles RNA) were recovered and treated with 2,5µl of proteinase K solution (600 mAU/ml) for 1 hour at 37°C in order to remove serum proteins that interfere with electrophoretic migration. Following the addition of 9 µl of denaturing gel loading buffer (1× TBE, 95% formamide, EDTA 10mM and bromophenol blue), samples were stored at −80°C. All serum-RNA samples were analyzed on 15%

polyacrylamide/urea 7M denaturing gel. The gel was stained with ethidium bromide and visualized by UV exposure.

3.11 ELONA (Enzyme-linked oligonucleotide assay) assay for CA-IX and human serum albumin

C96 maxisorp nunc-immunoplate (Thermo Fisher Scientific, Waltham, MA, USA) were left untreated or coated with 25nM of human serum albumin (HAS) (Sigma, St Louis, MO) or with 50nM of CA-IX in Coating/Washing buffer (20 mM Tris HCl pH 7.4; 150 mM NaCl; 1 mM $MnCl_2$; 0.5 mM $MgCl_2$; 2 mM $CaCl_2$) overnight at 4°C.
Wells were washed once with Coating/Washing buffer and blocked for 2 hours at room temperature (RT), with Coating/Washing buffer containing 5% non-fat dried milk. Following two washes with Coating/Washing buffer, the biotinylated 2'-F-RNA S-47s1 and S51s1 aptamers were heated at 95 °C for 5', snap-cooled on ice for 3min and allowed to warm up to 37°C for 10' and, then, incubated for 2 hours at room temperature at different concentrations (10-100-200-1000nM) in Coating/Washing buffer containing 1,6% non-fat milk . After three washes with Coating/Washing buffer, samples were incubated for 1 hour at room temperature with horseradish peroxidase (HRP)-conjugated Streptavidin (Thermo Fisher Scientific, Waltham, MA, USA) diluted 1:1000 in PBS.
Following four washes with PBS, signals were reveled with 3,3',5,5'-tetrametilbenzidina (TMB) substrate solution (Thermo Fisher Scientific, Waltham, MA, USA) and stopped with stop solution (H_2SO_4 0.16M) for TMB substrate (Thermo Fisher Scientific, Waltham, MA, USA). Absorbance at 450nm was measured with Multiskan FC Microplate Photometer (Thermo Fischer Scientific, Waltham, MA, USA).
As positive control of human serum albumin protein an anti-HSA biotinylated polyclonal antibody (concentration: 1:1000, Abcam; Cambridge, MA) was used.
Instead, as positive control of CAIX an anti-CAIX primary antibody (concentration: 1:1000, R&D) and finally with donkey anti goat as secondary antibody (concentration: 1:2000) was used.
The assays were performed in duplicate.

3.12 Flow cytometry analysis

CA-IX expression in COS7 transfected with human CA-IX plasmid was detected by anti-human CA-IX primary antibody (R&D Systems, Milan,

Italy). Alexa Fluor 488 donkey anti-goat IgG (Invitrogen, Milan, Italy) was used as secondary antibody. Cells were analyzed with FACS BD Accuri C6 (BD Biosciences, Franklin Lakes, New Jersey, USA). IgG antibody (Millipore, Burlington, MA, USA) was used as negative control.

4 RESULTS

4.1 CA-IX cell-SELEX design: two steps method

As shown in figure 15, CAIX cell-SELEX was divided in two different protocols called:

- Physiological cell-SELEX to find aptamers that recognize CA-IX physiologically induced;
- Specific cell-SELEX to find aptamers that recognize CA-IX with high specificity;

The Physiological cell-SELEX protocol exploited a cell line of triple negative cell line, called MDA-MB-231, treated with $CoCl_2$.
The MDA-MB-231 cell line was already characterized in hypoxic condition. It is negative for the second isoform of CAs expressed in cancer CAXII, but positive for CA-IX because it was essential to avoid the selection of aptamers for other CAs isoform.
In particular, the Physiological cell-SELEX protocol provides the MDA-MB-231 in normoxic condition for the counter-selection step, instead MDA-MB-231 treated with $CoCl_2$ for the selection step.
The Physiological cell-SELEX approach represents a valid and needful starting point to select aptamers for CA-IX, but even if the protocol avoids the selection of aptamers for CAXII isoform, the final pool will be enriched for every $CoCl_2$ target genes expressed by MDA-MB-231 cells, among them CA-IX.
Thus, in order to discard not specific CA-IX aptamers selected during the Physiological cell-SELEX protocol and sort only those binding CA-IX, a second approach was planned named Specific cell-SELEX.
In this case, the selection step of Specific cell-SELEX provides COS7 cells transiently transfected with human CA-IX cDNA (COS7-CA-IX) for the selection step, instead wild type COS7 cell line (COS7-WT) for the counter-selection.
Starting from 9^{th} pool obtained from the Physiological cell-SELEX, both the protocols (Physiological cell-SELEX and Specific cell-SELEX) were performed at the same time for three cycles (10/10a, 11/11a, 12/12a).
At the end, the matching of the pools obtained could represent a useful tool to find an aptamer binding only CA-IX in its physiological conformation.

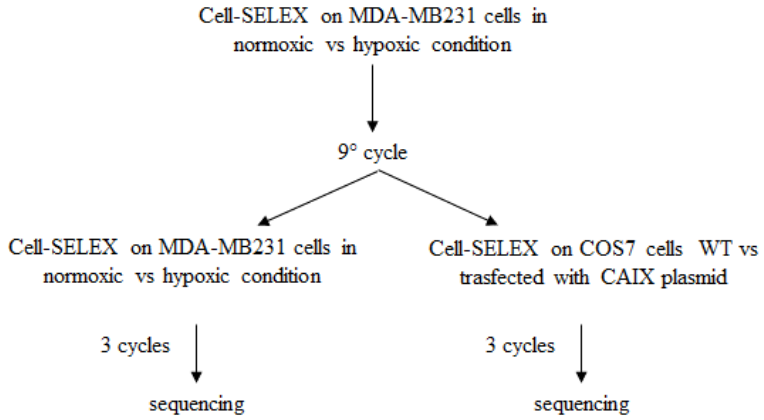

Fig. 15: Schematic design of the CA-IX cell-SELEX. The CA-IX cell-SELEX consists of two different protocols. (i) Twelve cycles of Physiological cell-SELEX on MDA-MB-231; (ii) three cycles of Specific cell-SELEX on COS7 cells, followed by the sequencing of both last cycles.

4.2 Physiological CA-IX expression set up and Physiological cell-SELEX

4.2.1 *In vitro* hypoxia induction

As first attempt, to design the anti-CAIX aptamer selection we address the choice of: 1. the best method to induce hypoxic condition; 2. the cell system to use as target.
Hypoxia can be induced *in vitro* by physical and chemical methods. The physical method is represented by the hypoxia incubator chamber that maintains low O_2 levels (1-5%). The hypoxia incubator chamber is the best way to reproduce and study the hypoxia phenotype *in vitro*. However, the hypoxia incubator chamber is not useful for every types of experiments because, as soon as oxygen enters in the chamber, the hypoxia is reduced.
Instead, the chemical methods exploits different types of molecules such as Cobalt (II) Chloride hexahydrate ($CoCl_2$), dimethyloxalylglycine (DMOG), desferrioxamin (DFO) and MG132.
Among them, Cobalt (II) Chloride hexahydrate ($CoCl_2 \cdot 6H_2O$, MW=237.9Da) mimics hypoxic condition blocking prolyl-hydroxylase domain (PHD) and the factor inhibiting HIF-1 (FIH) (Fig.16). Consequently, VHL tumour-suppressor protein cannot bind to not prolyl-hydroxylated HIF-1a; it promotes the stabilization and phosphorylation of HIF-1α.
At the end, the increase of HIF-1α levels allows its accumulation and subsequent nuclear translocation activating the transcription of HIF-1 target genes (such as CA-IX) and mimicking the low oxygen condition.

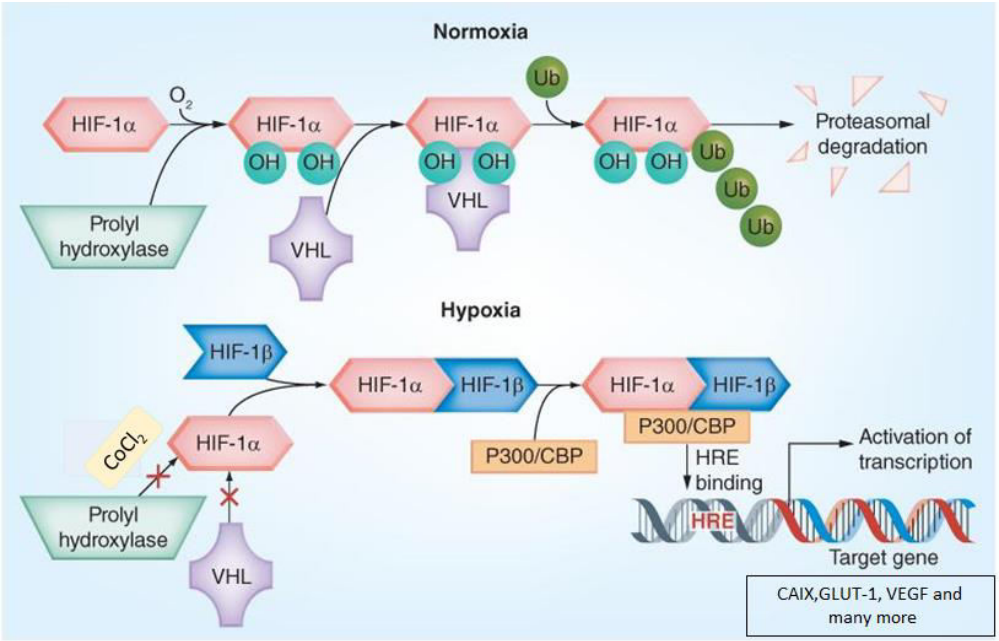

Fig. 16: $CoCl_2$ stabilises HIF-1α. The stability of HIF-1α protein is oxygen-sensitive. In normoxic condition two enzymes, prolyl-hydroxylase domain (PHD) and the factor inhibiting HIF-1 (FIH), promote the hydroxylation of proline and asparagine residues that is required for the binding of the VHL tumour-suppressor protein. That promotes the ubiquitination and degradation of HIF-1α. $CoCl_2$ inhibits PHD and FIH, thus VHL tumour-suppressor protein cannot bind to HIF-1α; HIF-1α can enter into the nucleus, bind to HIF-1β, p300 and CBP, allowing transcriptional activation of HIF-1 target genes. (Adapted from Burroughs SK et al. 2013)

However, $CoCl_2$ treatment can also modulate other proteins and pathways not HIF-1 dependent.

In this study, both the physical (hypoxia incubator chamber) and chemical methods ($CoCl_2$) were evaluated, in order to compare the induction of CA-IX.

The experiments were performed using the U87MG a human glioblastoma-derived cell line. Cells were seeded and treated with $CoCl_2$ 150µM at different times (1h, 6h, 24h) or were grown for 6, 24 and 48h in the hypoxia incubator chamber maintained at 5% oxygen levels.

After the cell lysis, the protein extracts were analysed by immunoblotting for HIF-1α and CA-IX expression.

The results showed different kinetic of HIF-1α induction between the two approaches examined. In fact, using the hypoxia incubator chamber HIF-1α was expressed by 6h until 48h, while using $CoCl_2$ its expression was

strongly induced at 6h then rapidly declines. In both conditions tested, CA-IX protein was induced at 24 hours (Fig. 17 a, b).

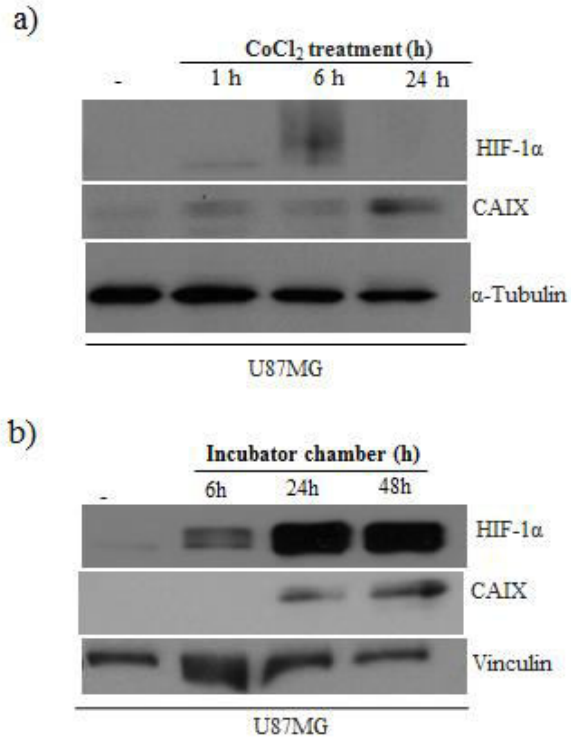

Fig. 17: Evaluation of CA-IX and HIF-1α using $CoCl_2$ treatment and hypoxia incubator chamber. a) U87MG cells were seeded and treated with 150μM of $CoCl_2$ for different times (1h, 6h, 24h) **b)** U87MG cells were seeded and left in hypoxia incubation chamber for 6h, 24h and 48h. Cells were collected and a Western blot was performed to evaluate HIF-1α (120Kda) and CA-IX (58Kda) expression. Tubulin (55Kda) and vinculin (120Kda) were used as housekeeping reference.

Based on the results above, the use of $CoCl_2$ was preferable for the SELEX procedure because it allows to open the culture plate/dish/flask and add treatments without changing the "hypoxic" conditions.
The selection of the cell line to use as target is another important feature for the success of the strategy. One key aspect is to prevent the isolation of aptamers for other CAs family, in particular CAXII, that is often overexpressed on cancer cell surface.
Basing on this consideration, U87MG cells were considered not the optimal target because they express, at the same time, CA-IX and CA-XII, when maintained in hypoxic condition [107].

On the contrary, previous reported data [108] showed that the triple negative breast cancer cell line, MDA-MB-231, in hypoxic condition is positive for CA-IX but negative for CA-XII expression.

4.2.2 Hypoxic like condition set up on MDA-MB-231 cells

To confirm the hypoxic-like phenotype and, consequently, the CA-IX expression, $CoCl_2$ was tested on MDA-MB-231 cell line.
The MDA-MB-231 cells were seeded and treated with 100, 150 and 200µM of $CoCl_2$ at different times (6, 24, and 48 h) (Fig.18).
Cells were recovered and Western blot assay was performed to evaluate:

1. HIF-1α expression levels, to assess its stabilization after $CoCl_2$ treatment;
2. CA-IX expression, to confirm its upregulation HIF-1 depending.

As expected, HIF-1 was expressed prior to CA-IX. In fact, the induction of HIF-1α was already visible at 6 hours upon the treatment, while the expression of CA-IX was appreciable starting from 24 hours, compared to normoxic cells (used as negative control), in all the conditions tested. The best induction of CA-IX protein on MDA-MB-231 cell line, was detected at 24 hours with 150µM of $CoCl_2$.

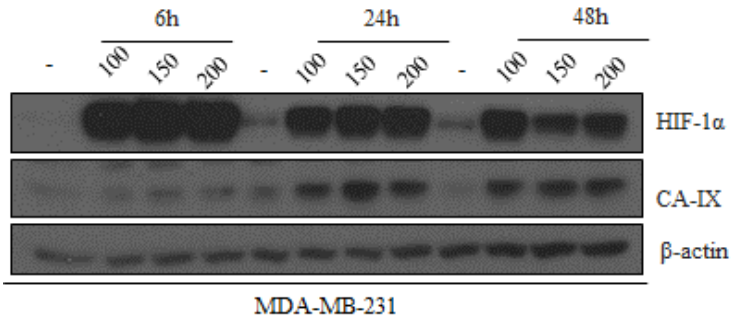

Fig. 18: Time and dose-response assay for CA-IX and HIF-1α expression. MDA-MB-231 cells were treated with increasing concentrations of $CoCl_2$ (100, 150, 200µM) for 6, 24, 48 hours. Cells were recovered and the Western blot was performed to evaluate CA-IX and HIF-1α expression; β-actin was used as housekeeping reference.

Moreover since the right localization on cell membrane surface of CAIX is the essential condition to select aptamers, an immunofluorescence assay was performed followed $CoCl_2$ at the optimal concentration and time identified (150µM for 24 hours).
MDA-MB-231 cells were seeded and treated with $CoCl_2$. The living cells were first incubated with anti-CA-IX primary antibody, then, fixed and incubated with Alexa-488-labeled secondary antibody.

Following several washes, the cells were visualized by confocal microscope in order to evaluate the CA-IX localization. Cells grown in normoxic conditions were used as negative control.
As shown in figure 19, the result indicated the presence of CAIX on the membrane surface compared to normoxic cells.

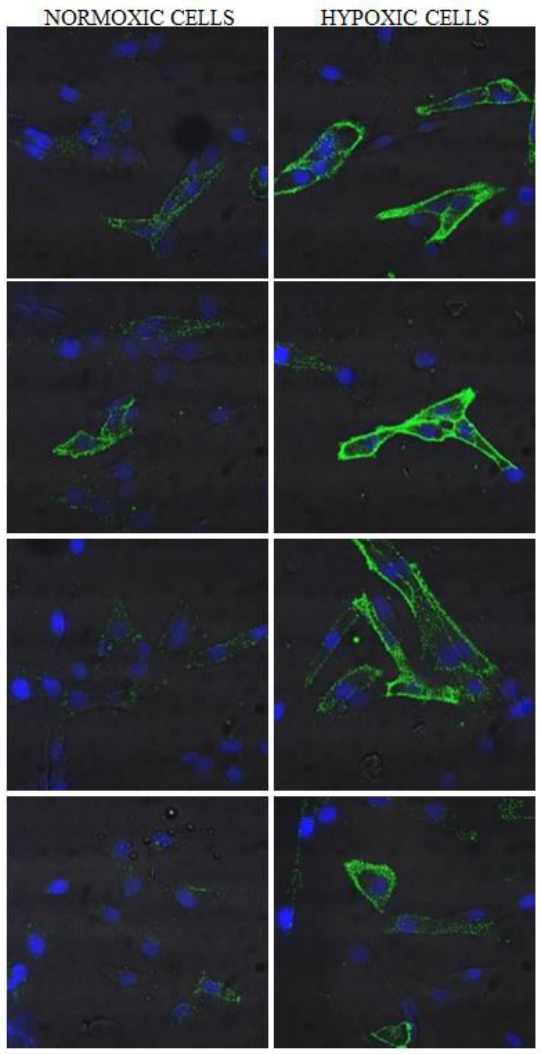

Fig.19: CA-IX expression on MDA-MB-231 cellular surface. MDA-MB-231 cells in normoxic condition or treated with 150µM of $CoCl_2$ for 24h were seeded, incubated with CA-IX primary antibody and then fixed. The Alexa-488-labeled secondary antibody was used to detect the fluorescence by confocal microscopy. The image shows four representative field of the same slide.

4.3.2 Physiological cell-SELEX design

In order to isolate specific ligands for the given condition, twelve rounds of Physiological cell-SELEX protocol were performed.
We used as target $CoCl_2$-induced MDA-MB-231 in the selection steps and normoxic MDA-MB-231 cells in the counter-selection steps.
The starting point was a library of RNA aptamers formed by a central degenerated sequence of 40 nucleotides flanked by two fixed regions. At each round, 2'Fluoro-Pyrimidines (2-F-Py) were incorporated in the RNA library instead of Pyrimidines in order to improve resistance of RNA molecules from degradation by serum nucleases.
At each round, the library was first incubated with MDA-MB-231 cells grown in normoxic condition to discard aptamers binding protein expressed. The unbound sequences were recovered and incubated on $CoCl_2$-induced MDA-MB-231 cells for the selection step (Fig.20). After several washings, the bound RNAs were recovered by total RNA extraction, retrotranscribed by RT-PCR followed by a mutagenic PCR (in presence of high concentration of nucleotides and magnesium), to increase library variability.
Finally, *in vitro* transcription was peroformed to obtain the new RNA pool for the next cycle.

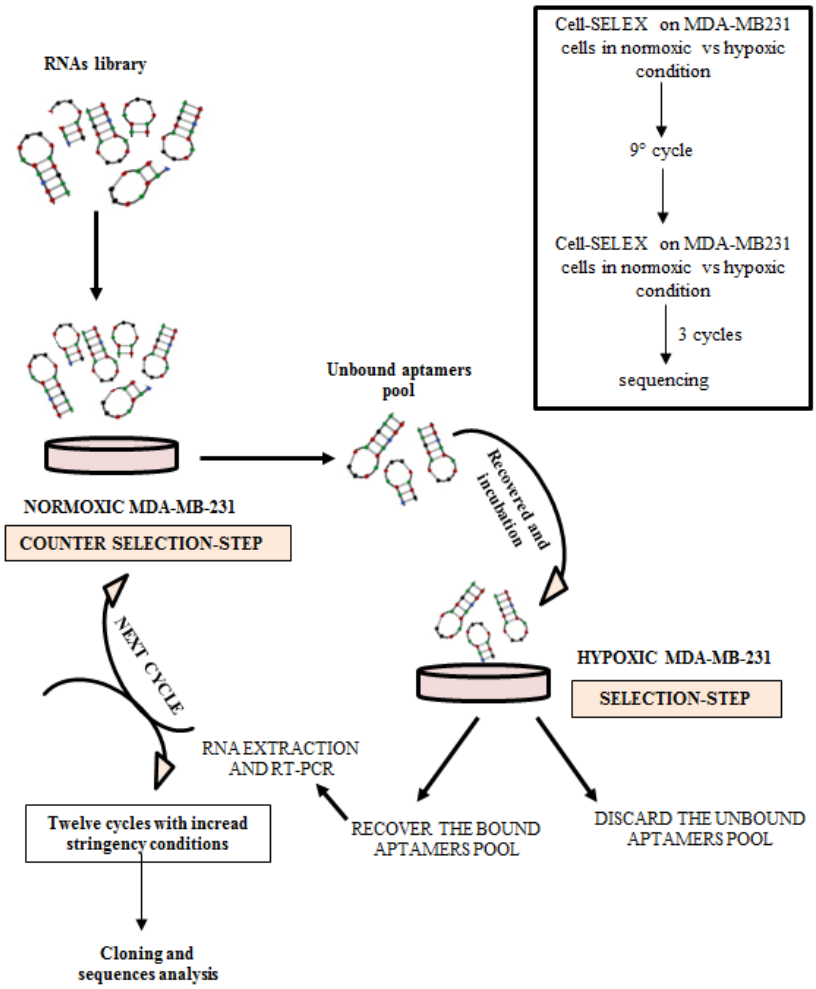

Fig. 20: Scheme of Physiological cell-SELEX. Each cycle is composed by a counter-selection step on normoxic MDA-MB-231 and a selection step on hypoxic-like MDA-MB-231. After twelve cycles with increased stringency conditions, the last cycle was cloned and sequenced.

During the Physiological cell-SELEX protocol, the selective pressure was progressively increased to select only the most promising aptamers by: (i) reducing cell confluence and incubation time to discard aptamers with low binding capability; (ii) increasing the washes number and adding polianionic competitor (yeast tRNA) to prevent unspecific binding (Table 3).

Cycle	Cell confluence 80%	RNA amount (pmol)	Incubation Time (min)	Washes number	Counter-selection number	Competitor (Yeast tRNA)	Pre-incubation with yeast tRNA
1	p150	600	30’	1	1	//	//
2	p150	600	30’	2	1	//	//
3	p150	600	30’	3	1	//	//
4	p150	600	30’	4	1	//	//
5	p100	600	30’	4	1	//	//
6	p100	600	30’	5	1	//	//
7	p100	600	15’	5	1	//	//
8	P100	600	15’	5	2	//	//
9	p60	600	15’	5	2	//	//
10	p35	600	15’	5	2	100 µg/ml	//
11	p35	600	15’	6	2	100 µg/ml	100 µg/ml
12	p35	600	15’	6	3	200 µg/ml	200 µg/ml

Table 3: Stringent conditions of Physiological cell-SELEX.

At each cycle, the library enrichment was checked by loading the PCR product on 12% acrylamide gel (Fig. 21a) and to control the hypoxic-like phenotype HIF-1α and CA-IX expression was evaluated by immunoblotting (Fig. 21b).

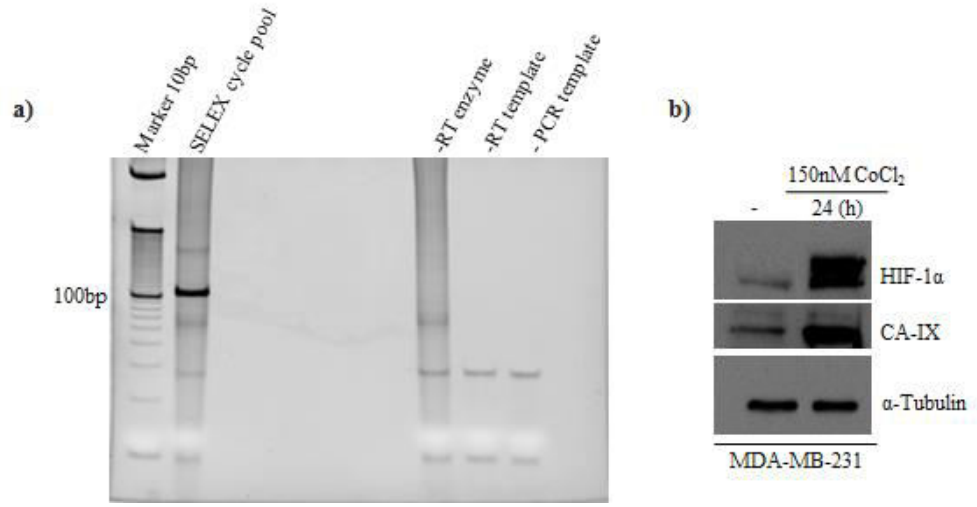

Fig. 21: cell-SELEX cycle on MDA-MB-231 cells: mutagenic PCR and immunoblotting. a) The mutagenic PCR control on 12% acrylamide gel, stained with ethidium bromide and visualized by UV. Sample "-template" represents the sample for RT or PCR without the template, whereas sample "–RT enzyme" is the reverse-transcription sample without the reverse-transcriptase enzyme; **b)** MDA-MB-231 cells in normoxic and hypoxic condition were collected to check HIF-1α a and CA-IX expression by immunoblotting.

After 12 rounds of selection, sequences were cloned with TOPO-TA cloning kit. The TOPO TA cloning reaction was performed and the product was used for the transformation of chemically competent bacteria DH5α.
White and light blue colonies were selected for DNA extraction by mini-prep kit. The DNA was analysed by electrophoresis on a 1% agarose gel supplemented with 0,05 μg/mL of Ethidium Bromide (Fig.22) and visualized by UV.

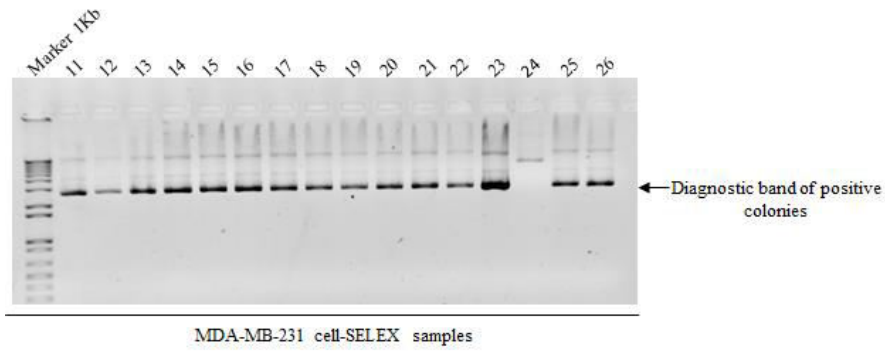

Fig. 22: Example of DNA plasmid. Samples from 11 to 26 were loaded on 1% agarose gel supplemented with 0,05 µg/mL of Ethidium Bromide (EtBr) and visualized by UV exposure. The different migration pattern is indicative of the fragment insertion.

One hundred aptamers were sequenced and grouped in families based on their primary sequence similarity. Sequences were analysed for enrichment by alignment and dendrogram visualization.

As shown in the figure 23, the dendrogram presented twelve couples of identical sequences (MA-13/40, -7/-15, -16/-18, -2/-21, -39/-76, -50/-96, 52/-58, -9/-70, -98/-82, -44/-90, -66/-97, -28/-100), that together cover 24% of all individual sequences obtained from the sequencing.

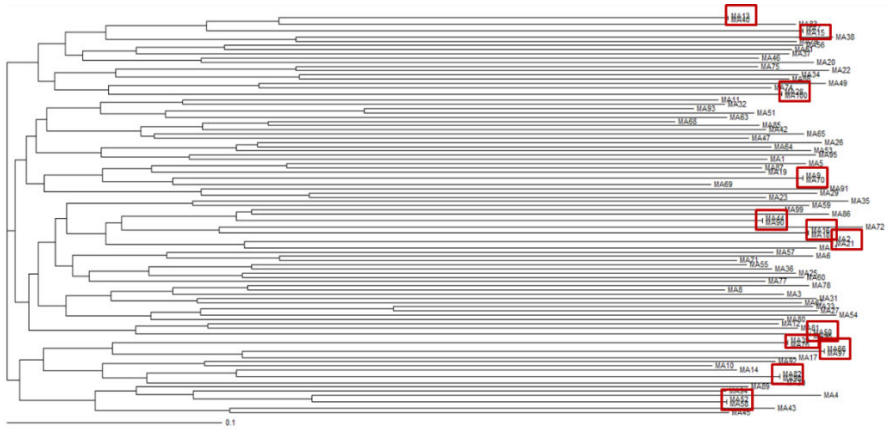

Fig.23: Physiological cell-SELEX analysis of individual sequences similarity. Dendrogram (by using MUSCLE algorithm) for visual classification of similarity among 100 individual sequences cloned after 12 rounds of selection. All couples are boxed in red.

4.4 CA-IX expression set up and Specific cell-SELEX design

4.4.1 Transfection of human CA-IX plasmid set up

After Physiological cell-SELEX, the pool of aptamers was enriched for all HIF-1 dependent proteins such as CA-IX, but also P-selectin, CXCR4, and many more (Table 4).

Role	Gene product
Vasomotor control	Adrenomedullin (AM) Nitric oxide synthase 2 (NOS2) α1B adrenergic receptor Endothelin 1 (ET1)
Angiogenesis	Vascular endothelial growth factor (VEGF) FLT1 (VEGF receptor 1, VEGFR1)
Erythropoiesis	Erythropoietin (EPO)
Iron metabolism	Transferrin Transferrin receptor Ceruloplasmin
Cell proliferation/ Cell cycle control	p21 (WAF1/CIP1) Insulin-like growth factor 2 (IGF2) IGFBP1, IGFBP2, IGFBP3
Cell death	NIP3, NIX
Energy metabolism	Glucose transporters 1 and 3 (GLUT1, GLUT3) Prolyl-4-hydroxylase α1 Phosphofructokinase L Lactate dehydrogenase A Aldolases A and C Pyruvate kinase M Enolase 1 Hexokinases 1 and 2 Glyceraldehyde phosphate dehydrogenase (GAPDH)
Miscellaneous	Plasminogen activator inhibitor (PAI1) Transforming growth factor β3 (TGFβ3) p35srj Haem oxygenase 1 Adenylate kinase 3 Phosphoglycerate kinase 1 Carbonic anhydrase 9 RTP801

Table 4: Genes regulated by HIF-1. HIF-1, binding the HRE sequence of many genes, regulates different pathways. (From Sharp FR et al. 2004)

Thus, a second cell-SELEX protocol was planned in order to sort only specific aptamers for CA-IX.
The protocol started from the 9 cycles of Physiological cell-SELEX and was composed by three cycles on COS7 cells, used as recipient cells, transiently transfected with human CA-IX-cDNA (COS7-CAIX).
As first attempt, the human CA-IX cDNA transfection condition was set up by
using two different concentrations of CA-IX cDNA were tested (1µg and 2µg).
The cells were collected at 24, 48 and 72h of transfection and lysed.
Protein levels were analysed by immunoblotting and the expression of CA-IX protein resulted highest at 24h upon transfection with both concentrations (Fig. 24a). For the Specific cell-SELEX protocol the lower concentration at 24 hours was selected because less toxic for the cells.
Farther, to evaluate the localization of CA-IX on membrane surface, a flow cytometry assay was performed using the condition selected (1µg of CA-IX human plasmid at 24h). The result showed a good percentage (around 40%) of CA-IX on membrane surface confirming that this condition can be used for the Specific cell-SELEX protocol (Fig. 24b).

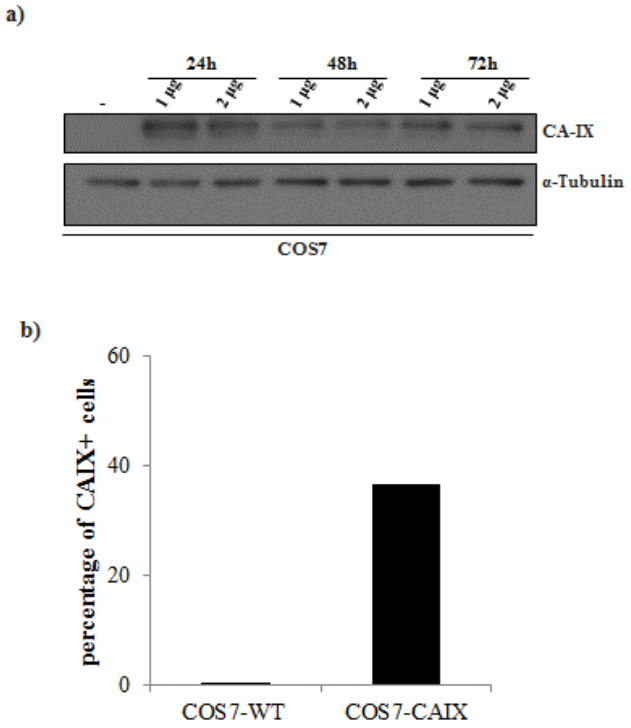

Fig. 24: CA-IX expression in COS7 cells. a) Following transfection with 1 and 2µg of CA-IX-cDNA, cells were collected at 24, 48 and 72h. Cell lysates were immunoblotted with anti-CA-IX antibody. α-tubulin was used as housekeeping reference. **b)** Following transfection with 1µg of CA-IX-cDNA, cells were collected at 24h. Cells incubated with anti-CA-IX primary antibody and then with Alexa-488-labeled secondary antibody, were analysed by flow cytometry. The percentage of CA-IX$^+$ cells was obtained subtracting the percentage of the control (IgG) value.

The low extracellular pH is important for the CA-IX conformation and function. Thus, in order to mimic *in vitro* acid microenvironment (pH 6.7-6.8), the COS7 cells after transfection were treated with MES (morpholinoethanesulfonic acid) buffer. Indeed, MES buffer ($C_6H_{13}NO_4S$) can be used to obtain the desired pH in a range from 5 to 7 resulting appropriate for our purpose.
The COS7 cells were seeded, transfected with CA-IX human plasmid (1µg) and treated with increasing concentrations of MES buffer (from 45 up to 90mM) for 30 minutes. The pH of the medium was measured by a pHmeter.

The result (Fig. 25) showed that the treatment with 60mM of MES buffer allowed to reach the extracellular pH maintained by CA-IX (around 6,8). This condition was used for Specific cell-SELEX.

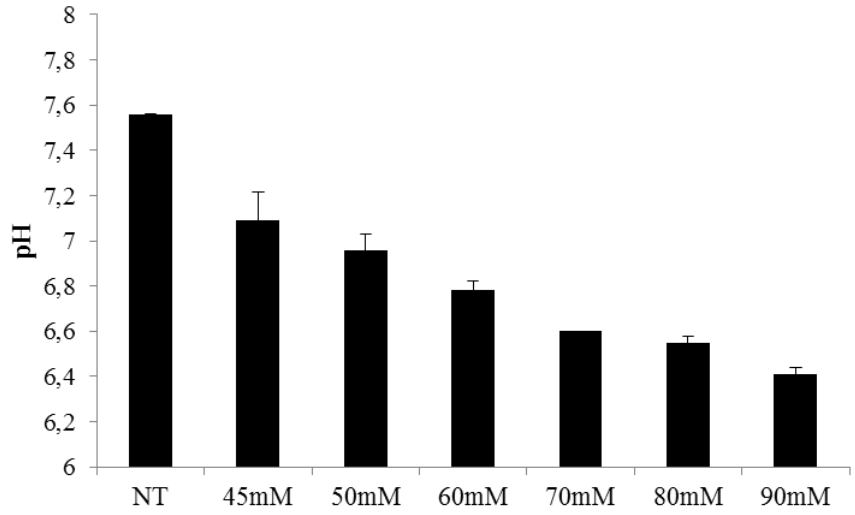

Fig. 25: Setting of extracellular environment acidification. MES buffer was incubated 45 up to 90mM at 30minutes on COS7 cells. The pH medium was measured with a pHmeter.

4.4.2 Specific cell-SELEX design

As shown in figure 26, the Specific cell-SELEX is composed by COS7 cell line transfected with CA-IX cDNA (COS7-CAIX) for the selection step and wild type COS7 cells (COS7-WT) for the counter-selection step. As starting point we used the pool coming from the ninth cycle of Physiological cell-SELEX and a total of three rounds were performed. At each round, the selective pressure was increased by performing two (cycles 10a, 11a) or three (cycle 12a) counter-selection steps on COS7-WT before the positive selection step (Table 5). In addition, in all three cycles, to prevent unspecific binding during the selection step, the library incubation was performed in presence of a polianionic competitor yeast tRNA. The tRNA was incubated with the library during the incubation time or it was also added before the library incubation as pre-treatment.

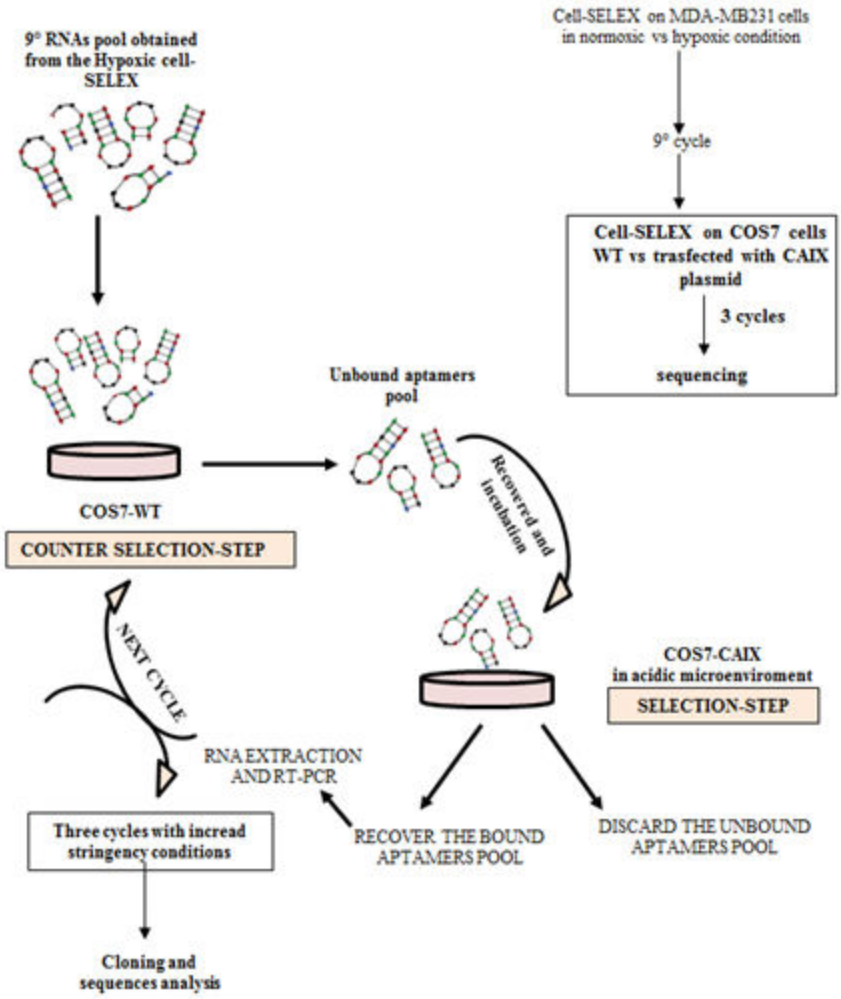

Fig. 26: Scheme of Specific cell-SELEX. Each cycle is composed by a counter-selection step on COS7-WT and a selection step on COS7-CAIX. After three cycles with increased stringency conditions, the last cycle was cloned and sequenced.

Cycle	Cell confluence 80%	RNA amount (pmol)	Incubation Time (min)	Washes number	Counter-selection number	Competitor (Yeast tRNA)	Pre-incubation with yeast tRNA
10a	p35	600	15'	5	2	100 µg/ml	//
11a	p35	600	15'	6	2	100 µg/ml	100 µg/ml
12a	p35	600	15'	6	3	200 µg/ml	200 µg/ml

Table 5: Stringent conditions for the Specific cell-SELEX.

After several washings, bound RNAs were recovered by total RNA extraction. Sequences enriched by the selection step were amplified by RT-PCR followed by mutagenic PCR and transcription before a new cycle of selection.
At each cycle, the pool amplification was checked (Fig. 27a) and CA-IX expression was analysed by immunoblotting (Fig.27b).

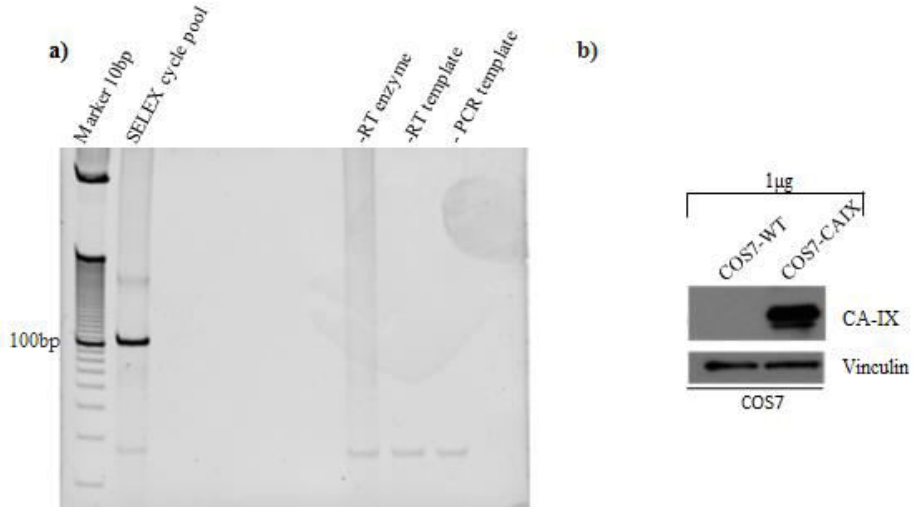

Fig. 27: Mutagenic PCR and immunoblotting relative to a Specific cell-SELEX cycle on COS7 cells. a) Mutagenic PCR control on 12% acrylamide gel stained with ethidium bromide and visualized by UV. **b)** Cells used for the cell-SELEX cycle were checked for CA-IX expression by immunoblotting. Vinculin was used as housekeeping reference.

The pool of the last SELEX cycle was cloned with TOPO TA kit and positive colonies (Fig.28) were sequenced.

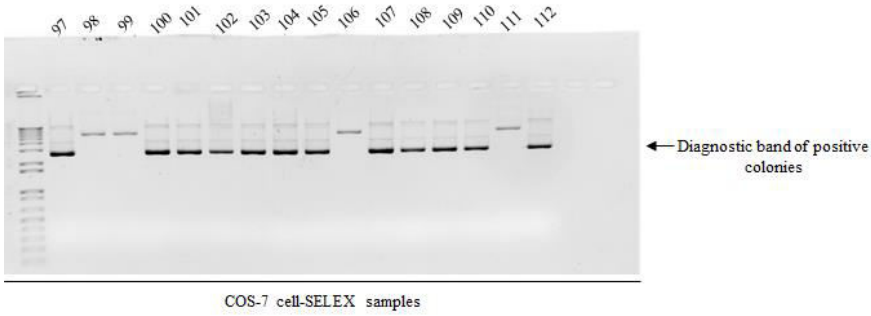

Fig. 28: Control of plasmid DNA extracted by mini-prep kit on 1% agarose gel. Samples from 97 to 112 were loaded on 1% agarose gel supplemented with 0,05µg/mL of Ethidium Bromide (EtBr) and visualized by UV exposure. The different migration pattern is indicative of the fragment insertion.

Ninety-eight sequences were sequenced from the 12a pool and aptamers grouped in families based on their primary sequence similarity. Sequences were analysed for enrichment by alignment and dendrogram visualization (Fig.29).

Six different groups of identical sequences (S-16/-8, -43/-100, -78/-47, -49/-74, -31/-69, S-23/-24/-34/-51) were found, that together represented more than 14% of all individual sequences obtained. One group of them, containing S-51, is composed by four identical sequences. Moreover, the S-51 group is also a part of an interesting enriched family that shares sequence similarity and represents the 9% of all the sequences analysed.

Specifically, the family is composed by:

1. a sub-group, containing S-51, composed by 4 sequences showing 100% of identity (S-23/-24/-34/-51);
2. three sequences (S-35,-52,-129) presenting 2 or 3 mismatches among them;
3. two sequences (S-22,-55) differing each other only for 2 nucleotides;

Basing on these considerations, the six couples and the enriched family were considered for further analyses.

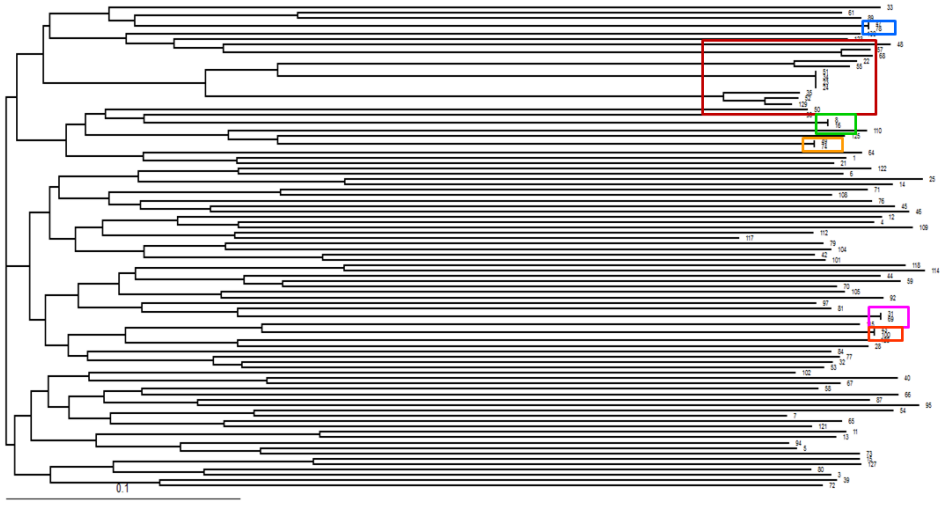

Fig. 29: Specific cell-SELEX analysis of individual sequences similarity.
Dendrogram (by using MUSCLE algorithm) for visual classification of similarity among 98 individual sequences cloned after 3 rounds of selection on COS7-CAIX and COS7-WT. Coloured boxes indicate the five couples of sequences; red box indicates the enriched family and the S-51 group that share sequence similarity.

4.5 Physiological cell-SELEX and Specific cell-SELEX: analyses of the sequences obtained

The most enriched family, obtained from Specific cell-SELEX, was analysed by CLUSTAL multiple alignment using MUltiple Sequence Comparison by Log- Expectation (MUSCLE) algorithm. It revealed 35% of identity among all the sequences of the enriched family.
In particular, the analysis showed a conserved consensus region of five nucleotides and many other identical nucleotides in all the sequences (fig.30a).
Additional analyses on the enriched family was done using the phylogenetic tree to analyse distance among the sequences (fig.30b) and Clustal 2.1 to evaluate the percent of identity (30c).
The last analysis showed a percent of identity among each sequence from 50-95%.

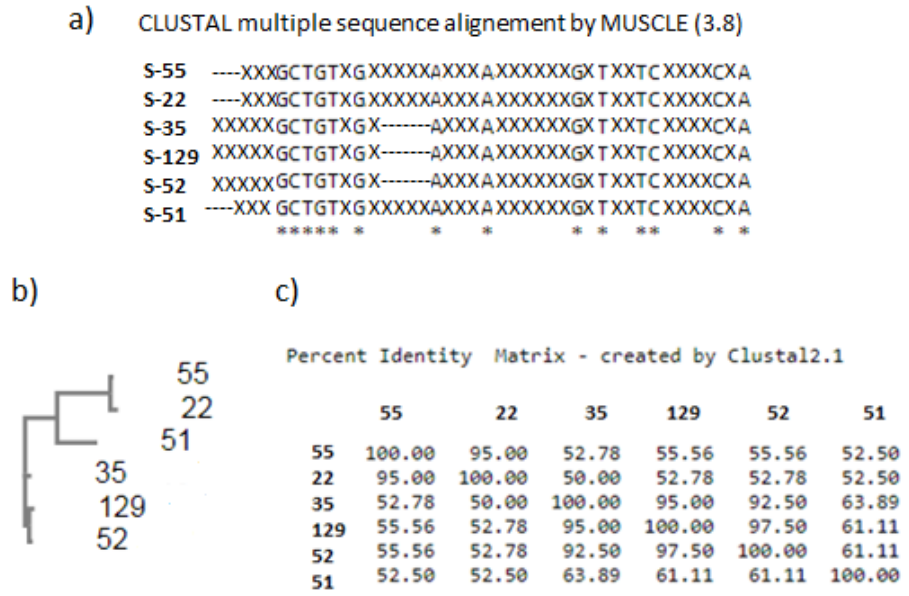

Fig. 30: Analyses of the most enriched sequences. a) CLUSTAL multiple sequence alignment by MUSCLE algorithm 3.8; **b)** Comparison of nucleotide sequences by Phylogenetic tree **c)** percent of identity by Clustal 2.1 .

In addition since we performed two different approaches (Physiological cell-SELEX and Specific cell-SELEX), we compared both dendrograms to analyse the presence of common sequences.
Although no identical sequences were found, the analyses revealed that one of the 12 couples obtained from the Physiological cell-SELEX (MA-39/76), maintains an identity of 27,5% with all the sequences of the most enriched family from Specific cell-SELEX.
Moreover, MA-39/76 shows the same consensus region of five nucleotides found in the enriched family (Fig.31a) and other common nucleotides along the sequence. The percent of identity of MA-39/76 with each individual sequence of the enriched family is around 44%-56% (Fig.31c).

Taken together, these data support the importance to test all these sequences.

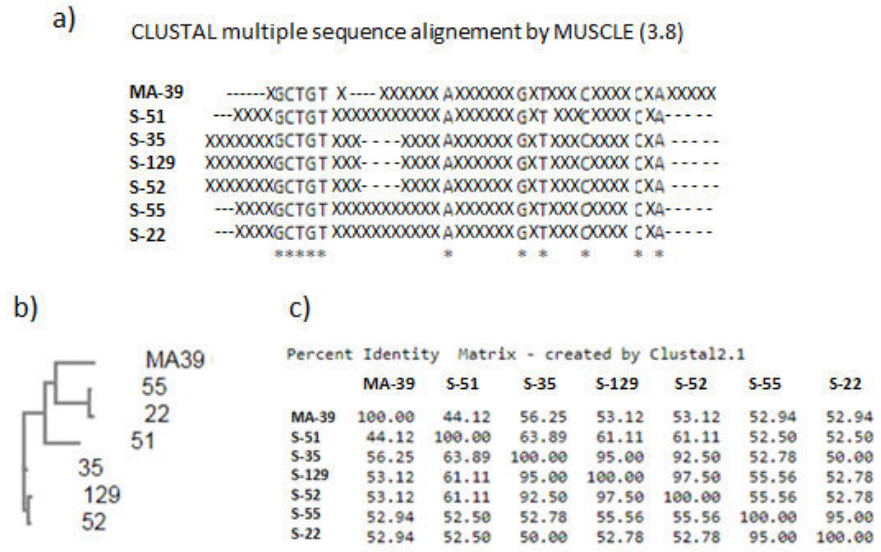

Fig. 31: Analyses of the MA-39/76 sequence compared to enriched family. a) CLUSTAL multiple sequence alignment by MUSCLE algorithm 3.8; **b)** Phylogenetic tree; **c)** Percent of identity achieved using Clustal 2.1.

4.6 Selection of the best aptamers for CA-IX

4.6.1 Binding of the enriched family

The binding capability of the enriched family was evaluated using one sequence of each group (S-35, -51, -55, -129 and MA-39).
The assay was performed comparing the sequences binding capability on COS7-CAIX over COS7-WT.
The COS7 cells were seeded and transfected with human CA-IX cDNA. After 24 hours, RNA sequences were incubated at 100nM for 15 minutes at 37°C, after pre-treatment with yeast tRNA at 200µg/mL and acid microenvironment induction with MES buffer (60mM). Samples were analysed by RT-qPCR to quantify the amount of bound aptamers. As shown in figure 32, S-51 and MA-39 sequences showed the best fold change over COS7-WT, whereas S-35 and S-55 were not able to discriminate between COS7-CAIX and COS7-WT.

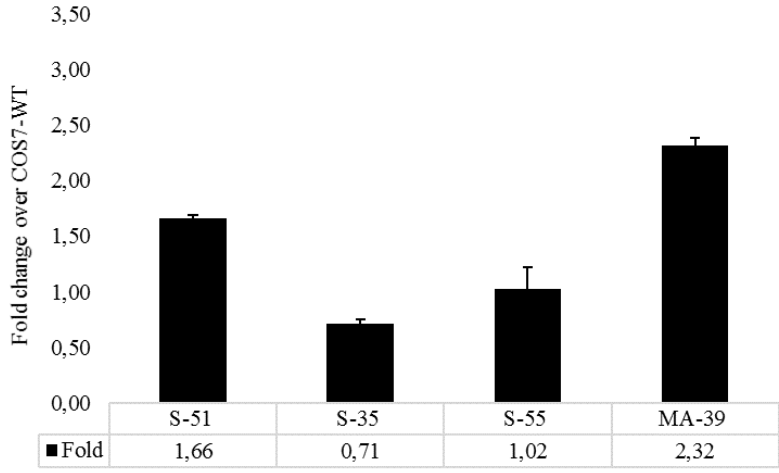

Fig. 32: RT-qPCR binding assay with sequences of the enriched family (S-35, -51, -55, -129 and MA-39) on COS7-CAIX cells. The binding assay, performed on COS7-CAIX cells (as positive cells) and COS7-WT (as negative cells), was analysed by RT-qPCR. In the graphic are indicate the fold change calculated over COS7 WT, arbitrarily equal to "1". The deviation standard was calculated on the RT-qPCR technical duplicates.

All these sequences were also tested on $CoCl_2$-induced MDA-MB-231 cells. Normoxic MDA-MB-231 were used as negative control (Fig.33).
As shown, the S-51 sequence was able to better discriminate between two different MDA-MB-231 phenotype.

Taken together, these results indicate that S-51 showed the best binding capability on all the CA-IX expressing cell lines tested.

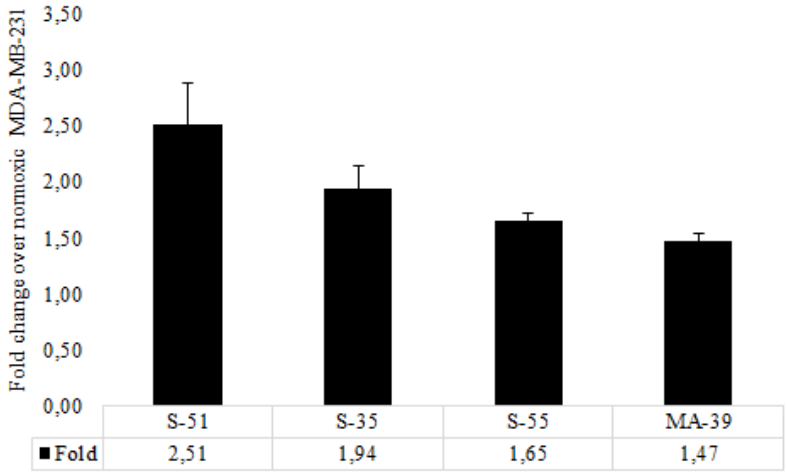

Fig. 33: RT-qPCR binding assay with sequences of the enriched family (S-35, -51, -55, -129 and MA-39) on hypoxic MDA-MB-231 cells. The binding assay, performed on MDA-MB-231cells in hypoxic condition (as positive cells) and MDA-MB-231cells in normoxic condition (as negative cells), was analysed by RT-qPCR. In the graphic are indicate the fold change calculated over MDA-MB-231cells in normoxic condition, arbitrarily equal to "1". The deviation standard was calculated on the RT-qPCR technical duplicates.

4.6.2 Binding of the enriched sequences

In addition to S-51 aptamer, the five couples found in the Specific cell-SELEX were analysed by RT-qPCR to evaluate the binding capability (S-16,-43,-47,-49,-69). COS7-WT and COS7-CAIX were used for the binding assay as reported above. Results were expressed as fold of binding of COS7-CAIX over COS7-WT. Among the sequences, the S-47, S-49, together with S-51, showed the best capability to bind COS7-CAIX (Fig.34), but S-49 was discarded because it showed the higher background on COS7-WT (not shown).

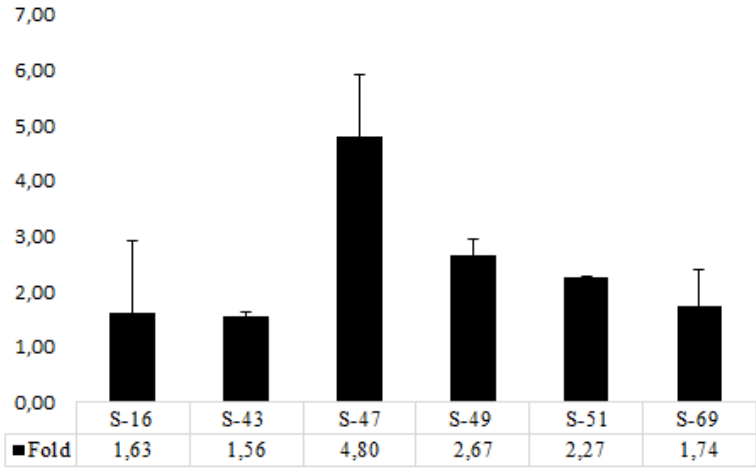

Fig.34: RT-qPCR binding assay for enriched sequences selected. The binding assay, performed on COS7-CAIX cells (as positive cells) and COS7-WT (as negative cells), was analysed by RT-qPCR. In the graphic are indicate the fold change calculated over COS7 WT, arbitrarily equal to "1". The deviation standard was calculated on the experimental duplicates.

4.7 Shortening of the best sequences

In order to obtain shorter sequences useful for imaging and therapeutic applications, using a rational approach based on their predicted secondary structure (by RNAfold), two truncated versions for each 84mer original aptamer were designed. Sequences were shortened isolating the region more structured (characterized by stems, loops, bulges and hairpins) possibly including the degenerate portion of the starting library and taking in consideration that the folding of the short versions was maintained.
The folding of the S-47 sequence exhibits two structured hairpins (Fig.35a). Thus, each hairpin was selected obtaining two short sequences, named S-47s1 and S-47s2 respectively of 25- and 34-mer, (Fig.35 b,c).

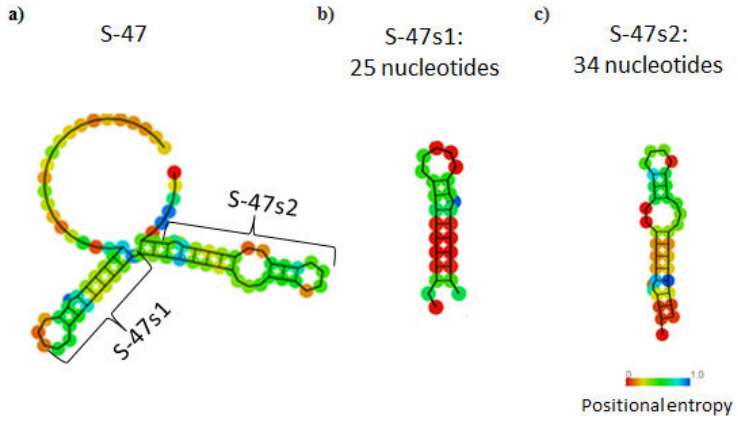

Fig. 35: Predicted secondary structure of S-47 selected aptamer anti-CA-IX and relative shortened versions by RNAfold program. a) S-47 long sequence and **b,c)** its shortened versions S-47s1 and S-47s2. The sequence colour is representative of positional entropy.

The S-51 sequence shows one hairpin. Thus, the sequence was cut obtaining two short sequences of different length, named S-51s1 and S-51s2 respectively of 24- and 52-mer (Fig.36).

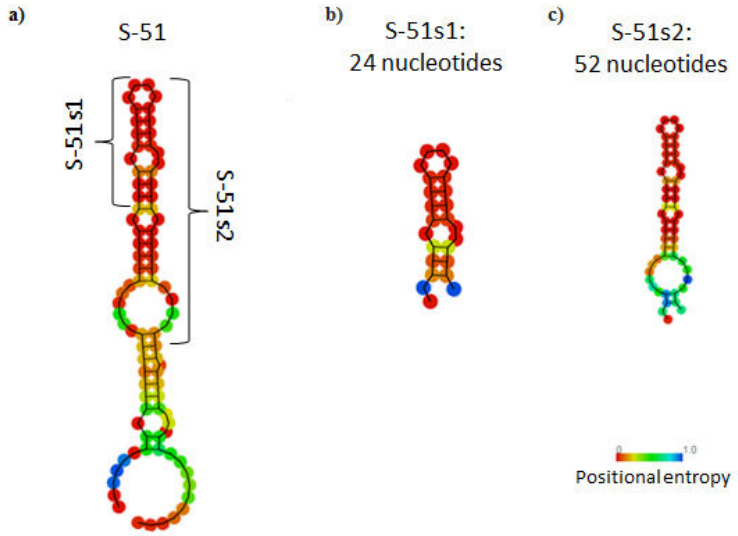

Fig. 36: Predicted secondary structure of S-51 selected aptamers anti-CA-IX and relative shortened versions by RNAfold program. S-51 long sequence and its shortened versions S-51s1 and S-51s2 secondary structures with lower free energy. The sequence colour is representative of positional entropy.

4.8 Binding of short sequences on CA-IX positive cells and on purified protein

To test the short aptamers binding capability the RT-qPCR binding assays were performed in duplicates maintaining the conditions used for the long aptamers screening.
A ratio was calculated comparing binding values of COS7-CAIX over COS7-WT.
As shown in the figure 37, in both two experiments performed the results showed a good discriminating ability of S-47s1 and S-51s1 compared to the other two short sequences designed (Fig.37).

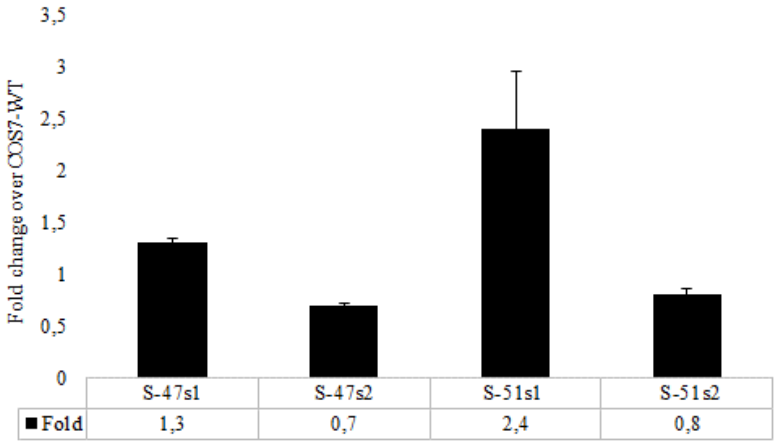

Fig. 37: RT-qPCR binding assay for four short sequences selected by SELEX anti-CA-IX. The binding assay, performed on COS7-CAIX cells (as positive cells) and COS7-WT (as negative cells), was analysed by RT-qPCR. In the graphic are indicate the fold change calculated over COS7 WT, arbitrarily equal to "1". The deviation standard was calculated on the experimental duplicates.

The best two aptamers (S-47s1 and S-51s1) were also tested on human CA-IX purified protein by ELONA assay to confirm definitively CA-IX as specific target.
The biotinylated S-47s1 and S-51s1 were incubated at 200nM concentrations on 96 well microtiter high binding plates previously coated or not-coated (blank) with 50nM of CA-IX.

As positive control was used a biotinylated polyclonal antibody anti CA-IX (1:1000).
As shown in figure 38, both the aptamers S-47s1 and S-51s1 bind to CA-IX human protein.

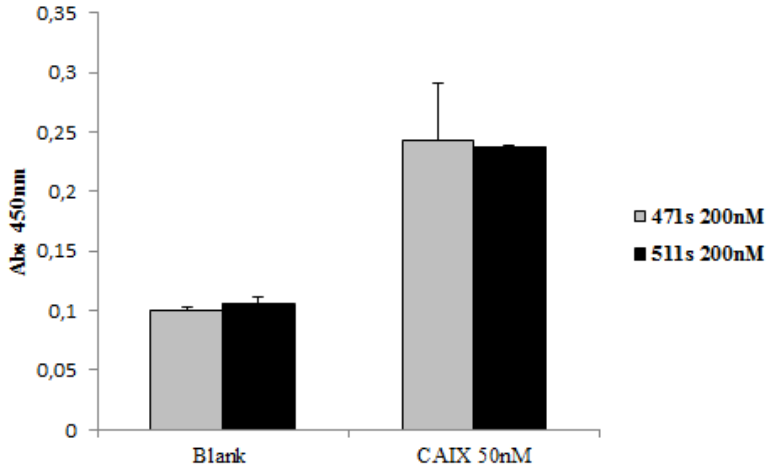

Fig.38: Binding evaluation for CA-IX of S-47s1 and S-51s1 aptamers. S-47s1 and S-51s1 200nM were incubated on CA-IX 50nM. Biotinylated polyclonal antibody anti-CA-IX (1:1000) was used as positive control.

4.9 Human serum stability of S-47s1 and S-51s1 aptamers

The stability in human serum was performed in triplicate using the best two aptamers selected, S-47s1 and S-51s1.
All the RNA aptamers tested are modified with 2-F-Py, in order to improve the nucleases resistance.
In order to analyse the half-life, 8 pmols of both of them were incubated at 37°C in human serum (87%) for different times (0, 1, 2, 4, 8, 12, 24, 48, 72 hours).
The samples were recovered at each time, loaded on 15% polyacrylamide/urea 7M denaturing gel and visualized at UV after ethidium bromide staining.
The result showed that S-47s1 and S-51s1 aptamer are extremely stable more than 72 hours (Fig.39).

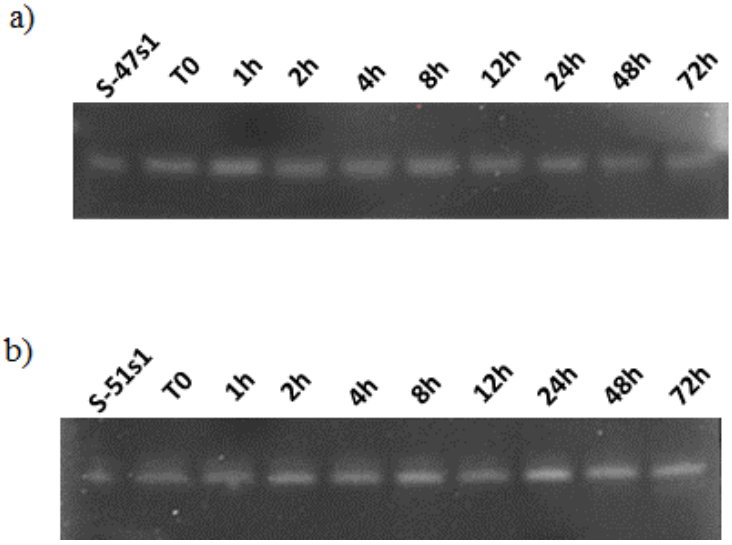

Fig.39: Human serum stability of S-47s1 and S-51s1 aptamers. Samples from T0 to 72 hour were loaded on 15% gel polyacrylamide/urea 7M denaturing gel and visualized at UV after Ethidium bromide staining. The first sample (S-47s1, S-51s1) for both gels indicates the sequence not treated with human serum to assess the right weight of the samples.

4.10 Kd Evaluation for HSA of S-47s1 and S-51s1 aptamers

In order to use the aptamer selected for *in vivo* purposes it is essential evaluate the albumin binding because the albumin is the most enriched protein in human plasm and could bind nucleic acids due to its charge.
For this reason, an ELONA assay using biotinylated S-47s1 and S-51s1 was performed to evaluate the binding to human serum albumin protein (HSA). The biotinylated sequences were incubated at increasing concentrations (1-10-100-1000nM) on 96 well microtiter high binding plates previously coated or not-coated (blank) with 25nM of HSA.
No binding was possible to calculate, indicating that S-47s1 and S-51s1 do not react with HSA up to 1000nM (Fig.40).
As positive control was used a biotinylated polyclonal antibody anti HSA (1:1000).

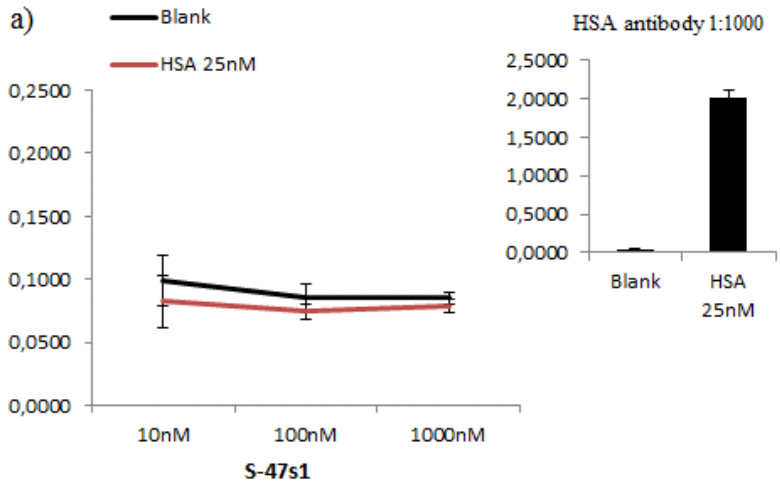

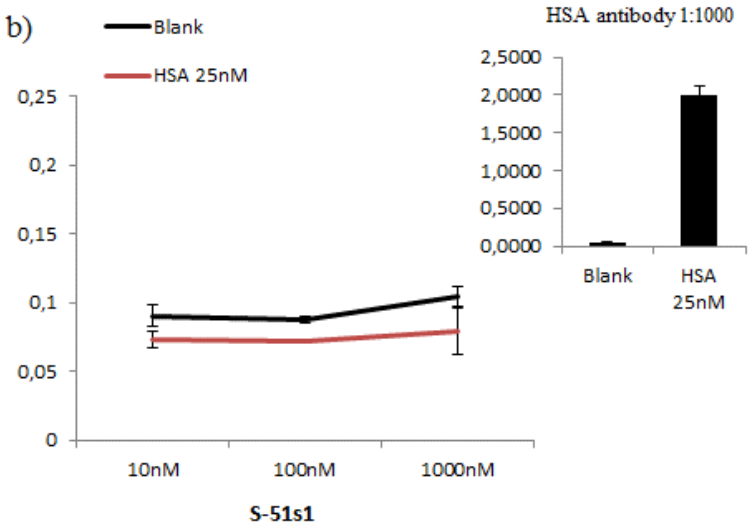

Fig.40: Kd evaluation for HSA of S-47s1 and S-51s1 aptamers. S-47s1 and S-51s1 10, 100, 1000nM were incubated on HSA 25nM. Biotinylated polyclonal antibody anti-HSA (1:1000) was used as positive control.

5. DISCUSSION

Hypoxia is a biological state of several types of solid tumours considered to be a negative prognostic factor in cancer, due to its association with an aggressive tumour phenotype and responsible for therapeutic resistance [109].
The hypoxia is involved in deregulation of cell cycle, reduction of apoptosis, shift in the metabolic pathway and resistance to treatments.
In order to detect tumour hypoxic sites different approaches, such as MRI methods, different nuclear medicine or PET analysis, have been explored [110]. However, there is not yet realized accurate and reproducible targeting agent able to selectively detect and/or inhibit the cancer cells survival in the hypoxic tumor regions.
From a biological point of view, the hypoxia is regulated by transcription factor HIF-1/2. It binds HRE regions and promotes the expression of several target genes [111,112]. Among the target genes, CA-IX is an emerging key biomarker. CA-IX belongs to carbonic anhydrases, a class of metalloenzymes able to catalyse the hydration of carbon dioxide to bicarbonate and protons. In particular, CA-IX and CA-XII, reducing the extracellular pH, promote the cancer progression [113, 114].
Thanks to its poorly expression in normal tissues, CA-IX is emerging as highly promising hypoxic target biomarker induced in the hypoxic regions of most tumours.
Until now, many classes of CAIX targeted therapeutic agents including small chemical compounds (inorganic anions, sulfonamide based compounds, phenols and coumarins [115] monoclonal antibodies (G250 [116], M75 [117] and mini-antibodies (A3 and CC7 [118]) have been described.
Despite some of them are promising agents, concerns remain about off-target toxicities due to interactions with intracellular CAs, and other extracellular CAs such as CAXII, which is also expressed in normal tissues.
To overcome the current limits, here we validated innovative strategy able to target a hypoxic marker CA-IX, using aptamers. Aptamers have become a new class of ligands for both therapeutic and diagnostic strategies. They are short oligonucleotides that can bind with high specificity to their target. Their advantages are easy production, low molecular weight, no immunogenicity and high specificity.
So far, nucleic acid molecules targeting HIF-1 have been conjugated to D-Fe3O4@PMn nanoparticles in order to detect hypoxia regions [119].

Despite promising, the limit of this approach is the unclear mechanism for the nanoparticles uptake.
The possibility to isolate aptamers able to target the hypoxic biomarker CA-IX can greatly improve aptamer-based strategies developed until now to detect hypoxia state. Being CA-IX an extracellular marker, it is an optimal target to develop tools allowing a direct detection without the need of sophisticated conjugation strategies.
Here we adopted a new SELEX protocol to generate high affinity aptamer ligands to target CA-IX-expressing cells. The use of living cells as targets for aptamer selection with high affinity (Kd= nM range) has been already applied to a wide range of systems [120]. It has been demonstrated the use of transfected cells to obtain aptamers for a specific target [121] and the possibility to select aptamers able to distinguish between closely related tumour cell phenotypes without a prior knowledge of the targeted epitopes [70].
In order to preserve as much as possible CAIX physiological context, reducing the possibility that the selected aptamer might not recognize the target *in vivo*, we designed an innovative cell-SELEX approach that combines two protocols.
The first goal was to preserve the functional conformation of CA-IX, thus, we started the selection plan by using a cell system in which CA-IX expression is inducible by mimicking hypoxic growth conditions. This protocol (named Physiological cell-SELEX) exploits the use of $CoCl_2$ that stabilizes the transcription factor HIF-1 and consequently promotes the expression of several target genes, including CAIX.
A triple negative breast cancer-derived cell line, MDA-MB-231, was used as target cells because they were already characterized in hypoxic condition for the induction of carbonic anhydrases expression. The MDA-MB-231 cells, under hypoxic condition, are positive for CA-IX but negative for CA-XII, avoiding the undesired selection of aptamers against CA-XII, another carbonic anhydrase isoform commonly expressed in cancer. At each cycle of Physiological cell-SELEX, the selection on hypoxic MDA-MB-231 was preceded by a counter-selection step on normoxic MDA-MB-231 depriving the pool of aptamers targeting proteins also expressed in normoxia. As starting library, we used a library of 2'F-Py RNAs because of their increased resistance to serum nucleases degradation.
This selection approach represents the first example of Physiological cell-SELEX to select aptamers for HIF-1 target genes including CA-IX. Although the protocol adopted would enrich for aptamers that recognize the physiological conformation of CA-IX, it would also enrich for

molecules able to discriminate between two different phenotype (normoxic *versus* hypoxic) binding other hypoxic-specific biomarkers. Therefore, by using the "Physiological-cell SELEX" we expect to generate aptamers for a set of targets, including but not limited to CA-IX.
In order to increase the selectivity for CA-IX, the Physiological cell-SELEX was combined to a second cell-SELEX protocol (called Specific cell-Selex) aimed to isolate among the pool enriched for hypoxic protein, those aptamers specific for CA-IX.
To this end, the pool coming from the 9^{th} cycle was subjected to three additional cycles on COS7 cell line transfected with an expression plasmid for the human CA-IX. To increase the selection pressure for CA-IX protein, the COS7 wild type cells were used as counter-selection step before each selection step.
At the same time, three extra cycles of Physiological cell-SELEX were made with two purposes: (i) to compare the results obtained from both cell-SELEX protocol; (ii) to have an enriched pool for every hypoxic target as a tool exploitable for future purposes. Finally, the last cycle of both cell-SELEX protocols (12 and 12a) was cloned and sequenced. Notably, among all the sequences tested, we identified two sequences (S-47 and S-51 aptamers) that effectively discriminated between CA-IX expressing and CA-IX negative cells.
In order to have an aptamer useful for *in vivo* purposes the aptamers must show an easy and cost effective production by chemical synthesis that also allows to make several type of modifications, such as the adding of the polyethylene glycol (PEG) or cholesterol tail, to improve the bioavailability.
Since long RNA sequences (> 60-70 nt) remain difficult to synthesize and have high costs of manufacturing, the
Selected sequences were further optimized by reducing their length to minimal functional sequences.
To this aim, from the original molecules of 84mer, S-47 and S-51 aptamers were truncated, using a rational approach based on their predicted secondary structure (by RNAfold), in two smaller sequences.
All the short aptamers (47-1s, 47-2s, 51-1s, 51-2s), were tested to confirm their binding to CA-IX-expressing cells leading to identify two short aptamer candidates, 47-1s and 51-1s, able to selectively bind the CA-IX positive cells.
The ability of these short aptamers to bind CA-IX was further investigated by ELONA assay confirming a good binding on CA-IX purified protein.

Moreover, in order to develop innovative tools for diagnosis and therapy the molecules selected must show (i) good stability in human serum to effectively reach the tumour; (ii) no binding to human albumin protein that, being the most abundant human protein in the blood, may hinder the achievement of tumour tissue.

Interestingly, the short candidate aptamers, 47-1s and 51-1s, resulted stable in 87% human serum more than 72 hours suggesting that the modifications used (2'F-Py) allows gaining a very impressive stability. In addition, no binding in the nanomolar range to human serum albumin was detected.

6. CONCLUSIONS

In conclusion, this study has identified new possible tools that are able to discriminate between CA-IX positive cells and CA-IX negative cells.
Considering that the hypoxia phenotype and CA-IX expressing cells are involved in chemotherapy resistance and poor prognosis, the aptamers identified in this study could have an important role in detecting only the hypoxic cells and acid microenvironment.
The study provide a new Selection strategy to successfully isolate aptamers with a very high specificity under physiological condition for *in vivo* applicability.
Although more studies are needed to better understand the usefulness of the selected molecules, taken together, our findings represent an initial development of novel aptamer-based tools for CA-IX detection.

7. REFERENCES

[1] Boveri T. Concerning the origin of malignant tumours by Theodor Boveri. Translated and annotated by Henry Harris. J Cell Sci. 2008 Jan;121 Suppl 1:1-84.
[2] Macconaill LE, Garraway LA. Clinical implications of the cancer genome. J Clin Oncol. 2010 Dec 10;28(35):5219-28.
[3] Hanahan D, Weinberg RA. The hallmarks of cancer. Cell. 2000 Jan 7;100(1):57-70.
[4] Hanahan D, Weinberg RA. Hallmarks of cancer: the next generation. Cell. 2011 Mar 4;144(5):646-74.
[5] Wigerup C, Påhlman S, Bexell D. Therapeutic targeting of hypoxia and hypoxia-inducible factors in cancer. Pharmacol Ther. 2016 Aug;164:152-69.
[6] Brown JM, Wilson WR. Exploiting tumour hypoxia in cancer treatment. Nat Rev Cancer. 2004 Jun;4(6):437-47.
[7] Vaupel P. The role of hypoxia-induced factors in tumor progression. Oncologist. 2004;9 Suppl 5:10-7.
[8] Thomlinson Rh, Gray Lh. The histological structure of some human lung cancers and the possible implications for radiotherapy. Br J Cancer. 1955 Dec;9(4):539-49.
[9] Brown JM. Evidence for acutely hypoxic cells in mouse tumours, and a possible mechanism of reoxygenation. Br J Radiol. 1979 Aug;52(620):650-6.
[10] Dewhirst MW, Ong ET, Braun RD, Smith B, Klitzman B, Evans SM, Wilson D. Quantification of longitudinal tissue pO2 gradients in window chamber tumours: impact on tumour hypoxia. Br J Cancer. 1999 Apr;79(11-12):1717-22.
[11] Chan N, Koritzinsky M, Zhao H, Bindra R, Glazer PM, Powell S, Belmaaza A, Wouters B, Bristow RG. Chronic hypoxia decreases synthesis of homologous recombination proteins to offset chemoresistance and radioresistance. Cancer Res. 2008 Jan 15;68(2):605-14.
[12] Luoto KR, Kumareswaran R, Bristow RG. Tumor hypoxia as a driving force in genetic instability. Genome Integr. 2013 Oct 24;4(1):5.
[13] Vaupel P, Mayer A. Hypoxia in tumors: pathogenesis-related classification, characterization of hypoxia subtypes, and associated biological and clinical implications. Adv Exp Med Biol. 2014;812:19-24.

[14] Rouschop KM, Ramaekers CH, Schaaf MB, Keulers TG, Savelkouls KG, Lambin P, Koritzinsky M, Wouters BG. Autophagy is required during cycling hypoxia to lower production of reactive oxygen species. Radiother Oncol. 2009 Sep;92(3):411-6.
[15] Koritzinsky M, Wouters BG. The roles of reactive oxygen species and autophagy in mediating the tolerance of tumor cells to cycling hypoxia. Semin Radiat Oncol. 2013 Oct;23(4):252-61.
[16] Kato Y, Yashiro M, Fuyuhiro Y, Kashiwagi S, Matsuoka J, Hirakawa T, Noda S, Aomatsu N, Hasegawa T, Matsuzaki T, Sawada T, Ohira M, Hirakawa K. Effects of acute and chronic hypoxia on the radiosensitivity of gastric and esophageal cancer cells. Anticancer Res. 2011 Oct;31(10):3369-75.
[17] Bellot G, Garcia-Medina R, Gounon P, Chiche J, Roux D, Pouysségur J, Mazure NM. Hypoxia-induced autophagy is mediated through hypoxia-inducible factor induction of BNIP3 and BNIP3L via their BH3 domains. Mol Cell Biol. 2009 May;29(10):2570-81.
[18] Reynolds TY, Rockwell S, Glazer PM. Genetic instability induced by the tumor microenvironment. Cancer Res. 1996 Dec 15;56(24):5754-7.
[19] Bersten DC, Sullivan AE, Peet DJ, Whitelaw ML. bHLH-PAS proteins in cancer. Nat Rev Cancer. 2013 Dec;13(12):827-41.
[20] Ivan M, Kondo K, Yang H, Kim W, Valiando J, Ohh M, Salic A, Asara JM, Lane WS, Kaelin WG Jr. HIFalpha targeted for VHL-mediated destruction by proline hydroxylation: implications for O2 sensing. Science. 2001 Apr 20;292(5516):464-8.
[21] Semenza GL. Hypoxia-inducible factors: mediators of cancer progression and targets for cancer therapy. Trends Pharmacol Sci. 2012 Apr;33(4):207-14. doi: 10.1016/j.tips.2012.01.005.
[22] Cecchi A, Hulikova A, Pastorek J, Pastoreková S, Scozzafava A, Winum JY, Montero JL, Supuran CT. Carbonic anhydrase inhibitors. Design of fluorescent sulfonamides as probes of tumor-associated carbonic anhydrase IX that inhibit isozyme IX-mediated acidification of hypoxic tumors. J Med Chem. 2005 Jul 28;48(15):4834-41.
[23] Türeci O, Sahin U, Vollmar E, Siemer S, Göttert E, Seitz G, Parkkila AK, Shah GN, Grubb JH, Pfreundschuh M, Sly WS. Human carbonic anhydrase XII: cDNA cloning, expression, and chromosomal localization of a carbonic anhydrase gene that is overexpressed in some renal cell cancers. Proc Natl Acad Sci U S A. 1998 Jun 23;95(13):7608-13.
[24] Pastoreková S, Závadová Z, Kostál M, Babusíková O, Závada J. A novel quasi-viral agent, MaTu, is a two-component system. Virology. 1992 Apr;187(2):620-6.

[25] Alvarez BV, Vilas GL, Casey JR. Metabolon disruption: a mechanism that regulates bicarbonate transport. EMBO J. 2005 Jul 20;24(14):2499-511. Epub 2005 Jun 30.
[26] Höckel M, Vaupel P. Tumor hypoxia: definitions and current clinical, biologic, and molecular aspects. J Natl Cancer Inst. 2001 Feb 21;93(4):266-76.
[27] Wykoff CC, Beasley NJ, Watson PH, Turner KJ, Pastorek J, Sibtain A, Wilson GD, Turley H, Talks KL, Maxwell PH, Pugh CW, Ratcliffe PJ, Harris AL. Hypoxia-inducible expression of tumor-associated carbonic anhydrases. Cancer Res. 2000 Dec 15;60(24):7075-83.
[28] Pastorekova S, Parkkila S, Pastorek J, Supuran CT. Carbonic anhydrases: current state of the art, therapeutic applications and future prospects. J Enzyme Inhib Med Chem. 2004 Jun;19(3):199-229.
[29] Semenza GL. HIF-1 mediates metabolic responses to intratumoral hypoxia and
oncogenic mutations. J Clin Invest. 2013 Sep;123(9):3664-71. doi: 10.1172/JCI67230.
[30] Muz B, de la Puente P, Azab F, Azab AK. The role of hypoxia in cancer progression, angiogenesis, metastasis, and resistance to therapy. Hypoxia (Auckl). 2015 Dec 11;3:83-92.
[31] Köhler K, Hillebrecht A, Schulze Wischeler J, Innocenti A, Heine A, Supuran CT, Klebe G. Saccharin inhibits carbonic anhydrases: possible explanation for its unpleasant metallic aftertaste. Angew Chem Int Ed Engl. 2007;46(40):7697-9.
[32] Supuran CT. Carbonic anhydrase inhibitors and activators for novel therapeutic applications. Future Med Chem. 2011 Jul;3(9):1165-80.
[33] Krishnamurthy VM, Kaufman GK, Urbach AR, Gitlin I, Gudiksen KL, Weibel DB, Whitesides GM. Carbonic anhydrase as a model for biophysical and physical-organic studies of proteins and protein-ligand binding. Chem Rev. 2008
Mar;108(3):946-1051.
[34] De Simone G, Vitale RM, Di Fiore A, Pedone C, Scozzafava A, Montero JL, Winum JY, Supuran CT. Carbonic anhydrase inhibitors: Hypoxia-activatable sulphonamides incorporating disulfide bonds that target the tumor-associated isoform IX. J Med Chem. 2006 Sep 7;49(18):5544-51.
[35] Winum JY, Temperini C, El Cheikh K, Innocenti A, Vullo D, Ciattini S, Montero JL, Scozzafava A, Supuran CT. Carbonic anhydrase inhibitors: clash with Ala65 as a means for designing inhibitors with low affinity for the ubiquitous isozyme II, exemplified by the crystal structure of the topiramate sulfamide analogue. J Med

Chem. 2006 Nov 30;49(24):7024-31.
[36] Garaj V, Puccetti L, Fasolis G, Winum JY, Montero JL, Scozzafava A, Vullo D, Innocenti A, Supuran CT. Carbonic anhydrase inhibitors: synthesis and inhibition of cytosolic/tumor-associated carbonic anhydrase isozymes I, II, and IX with sulfonamides incorporating 1,2,4-triazine moieties. Bioorg Med Chem Lett. 2004 Nov 1;14(21):5427-33.
[37] Ivanov SV, Kuzmin I, Wei MH, Pack S, Geil L, Johnson BE, Stanbridge EJ, Lerman MI. Down-regulation of transmembrane carbonic anhydrases in renal cell carcinoma cell lines by wild-type von Hippel-Lindau transgenes. Proc Natl Acad Sci U S A. 1998 Oct 13;95(21):12596-601.
[38] Pastoreková S, Závadová Z, Kostál M, Babusíková O, Závada J. A novel quasi-viral agent, MaTu, is a two-component system. Virology. 1992 Apr;187(2):620-6.
[39] Uemura H, Nakagawa Y, Yoshida K, Saga S, Yoshikawa K, Hirao Y, Oosterwijk E. MN/CA IX/G250 as a potential target for immunotherapy of renal cell carcinomas. Br J Cancer. 1999 Oct;81(4):741-6.
[40] Wykoff CC, Beasley N, Watson PH, Campo L, Chia SK, English R, Pastorek J, Sly WS, Ratcliffe P, Harris AL. Expression of the hypoxia-inducible and tumor-associated carbonic anhydrases in ductal carcinoma in situ of the breast. Am J Pathol. 2001 Mar;158(3):1011-9.
[41] Kopacek J, Barathova M, Dequiedt F, Sepelakova J, Kettmann R, Pastorek J, Pastorekova S. MAPK pathway contributes to density- and hypoxia-induced expression of the tumor-associated carbonic anhydrase IX. Biochim Biophys Acta. 2005 May 25;1729(1):41-9.
[42] Holotnakova T, Tylkova L, Takacova M, Kopacek J, Petrik J, Pastorekova S, Pastorek J. Role of the HBx oncoprotein in carbonic anhydrase 9 induction. J Med Virol. 2010 Jan;82(1):32-40.
[43] Takacova M, Holotnakova T, Barathova M, Pastorekova S, Kopacek J, Pastorek J. Src induces expression of carbonic anhydrase IX via hypoxia-inducible factor 1. Oncol Rep. 2010 Mar;23(3):869-74.
[44] Stillebroer AB, Mulders PF, Boerman OC, Oyen WJ, Oosterwijk E. Carbonic anhydrase IX in renal cell carcinoma: implications for prognosis, diagnosis, and therapy. Eur Urol. 2010 Jul;58(1):75-83.
[45] Beasley NJ, Wykoff CC, Watson PH, Leek R, Turley H, Gatter K, Pastorek J, Cox GJ, Ratcliffe P, Harris AL. Carbonic anhydrase IX, an endogenous hypoxia marker, expression in head and neck squamous cell carcinoma and its relationship to hypoxia, necrosis, and microvessel density. Cancer Res. 2001 Jul 1;61(13):5262-7.

[46] Koukourakis MI, Pitiakoudis M, Giatromanolaki A, Tsarouha A, Polychronidis A, Sivridis E, Simopoulos C. Oxygen and glucose consumption in gastrointestinal adenocarcinomas: correlation with markers of hypoxia, acidity and anaerobic glycolysis. Cancer Sci. 2006 Oct;97(10):1056-60.
[47] Rajaganeshan, R., Prasad, R.,Guillou,P.J., Scott,N., Poston,G., andJayne,D.G.(2009).Expression patterns of hypoxic markers at the invasive e margin of col-orectal cancers and liver metastases. Eur.J.Surg.Oncol. 35, 1286–1294.doi: 10.1016/j.ejso.2009.05.008
[48] Kim S, Jung WH, Koo JS. The Expression of Glut-1, CA-IX, and MCT4 in Mucinous Carcinoma. J Breast Cancer. 2013 Jun;16(2):146-51.
[49] Dubois L, Peeters S, Lieuwes NG, Geusens N, Thiry A, Wigfield S, Carta F, McIntyre A, Scozzafava A, Dogné JM, Supuran CT, Harris AL, Masereel B, Lambin P. Specific inhibition of carbonic anhydrase IX activity enhances the in vivo therapeutic effect of tumor irradiation. Radiother Oncol. 2011 Jun;99(3):424-31.
[50] Dubois L, Peeters SG, van Kuijk SJ, Yaromina A, Lieuwes NG, Saraya R, Biemans R, Rami M, Parvathaneni NK, Vullo D, Vooijs M, Supuran CT, Winum JY, Lambin P. Targeting carbonic anhydrase IX by nitroimidazole based sulfamides enhances the therapeutic effect of tumor irradiation: a new concept of dual targeting drugs. Radiother Oncol.2013Sep;108(3):523-8.
[51] McIntyre A, Patiar S, Wigfield S, Li JL, Ledaki I, Turley H, Leek R, Snell C, Gatter K, Sly WS, Vaughan-Jones RD, Swietach P, Harris AL. Carbonic anhydrase IX promotes tumor growth and necrosis in vivo and inhibition enhances anti-VEGF therapy. Clin Cancer Res. 2012 Jun 1;18(11):3100-11.
[52] Saarnio J, Parkkila S, Parkkila AK, Haukipuro K, Pastoreková S, Pastorek J, Kairaluoma MI, Karttunen TJ. Immunohistochemical study of colorectal tumors for expression of a novel transmembrane carbonic anhydrase, MN/CA IX, with potential value as a marker of cell proliferation. Am J Pathol. 1998 Jul;153(1):279-85.
[53] Závada J, Závadová Z, Pastoreková S, Ciampor F, Pastorek J, Zelník V. Expression of MaTu-MN protein in human tumor cultures and in clinical specimens. Int J Cancer. 1993 May 8;54(2):268-74.
[54] Wojtkowiak JW, Rothberg JM, Kumar V, Schramm KJ, Haller E, Proemsey JB, Lloyd MC, Sloane BF, Gillies RJ. Chronic autophagy is a cellular adaptation to tumor acidic pH microenvironments. Cancer Res. 2012 Aug 15;72(16):3938-47.
[55] Hermann T, Patel DJ. Adaptive recognition by nucleic acid aptamers. Science.2000 Feb 4;287(5454):820-5.

[56] Tucker WO, Shum KT, Tanner JA. G-quadruplex DNA aptamers and their ligands: structure, function and application. Curr Pharm Des. 2012;18(14):2014-26.
[57]. Dua P, Kim S, Lee DK. Nucleic acid aptamers targeting cell-surface proteins. Methods. 2011 Jun;54(2):215-25.
[58] Keefe AD, Cload ST. SELEX with modified nucleotides. Curr Opin Chem Biol. 2008 Aug;12(4):448-56.
[59] Foy JW, Rittenhouse K, Modi M, Patel M. Local tolerance and systemic safety of pegaptanib sodium in the dog and rabbit. J Ocul Pharmacol Ther. 2007 Oct;23(5):452-66.
[60] Higashimoto Y, Matsui T, Nishino Y, Taira J, Inoue H, Takeuchi M, Yamagishi S. Blockade by phosphorothioate aptamers of advanced glycation end products-induced damage in cultured pericytes and endothelial cells. Microvasc Res. 2013 Nov;90:64-70.
[61] Bates PJ, Laber DA, Miller DM, Thomas SD, Trent JO. Discovery and development of the G-rich oligonucleotide AS1411 as a novel treatment for cancer. Exp Mol Pathol. 2009 Jun;86(3):151-64.
[62] Lauridsen LH, Rothnagel JA, Veedu RN. Enzymatic recognition of 2'-modified ribonucleoside 5'-triphosphates: towards the evolution of versatile aptamers. Chembiochem. 2012 Jan 2;13(1):19-25.
[63] Ellington AD, Szostak JW. In vitro selection of RNA molecules that bind specific ligands. Nature. 1990 Aug 30;346(6287):818-22.
[64] Eulberg D, Buchner K, Maasch C, Klussmann S. Development of an automated in vitro selection protocol to obtain RNA-based aptamers: identification of a biostable substance P antagonist. Nucleic Acids Res. 2005 Mar 3;33(4):e45.
[65] Zhu G, Ye M, Donovan MJ, Song E, Zhao Z, Tan W. Nucleic acid aptamers: an emerging frontier in cancer therapy. Chem Commun (Camb). 2012 Nov 4;48(85):10472-80.
[66] Chen HW, Medley CD, Sefah K, Shangguan D, Tang Z, Meng L, Smith JE, Tan W. Molecular recognition of small-cell lung cancer cells using aptamers. ChemMedChem. 2008 Jun;3(6):991-1001.
[67] Shangguan D, Li Y, Tang Z, Cao ZC, Chen HW, Mallikaratchy P, Sefah K, Yang CJ, Tan W. Aptamers evolved from live cells as effective molecular probes for cancer study. Proc Natl Acad Sci U S A. 2006 Aug 8;103(32):11838-43.
[68] Sefah K, Meng L, Lopez-Colon D, Jimenez E, Liu C, Tan W. DNA aptamers as molecular probes for colorectal cancer study. PLoS One. 2010 Dec 10;5(12):e14269.

[69] Ye M, Hu J, Peng M, Liu J, Liu J, Liu H, Zhao X, Tan W. Generating aptamers by cell-SELEX for applications in molecular medicine. Int J Mol Sci. 2012;13(3):3341-53.
[70] Cerchia L, Esposito CL, Jacobs AH, Tavitian B, de Franciscis V. Differential SELEX in human glioma cell lines. PLoS One. 2009 Nov 24;4(11):e7971.
[71] Guo KT, Schäfer R, Paul A, Ziemer G, Wendel HP. Aptamer-based strategies for stem cell research. Mini Rev Med Chem. 2007 Jul;7(7):701-5.
[72] Mi, J. et al. In vivo selection of tumor targeting RNA motifs. Nat Chem Biol 2010, 6(1):22-24.
[73] Raddatz MS, Dolf A, Endl E, Knolle P, Famulok M, Mayer G. Enrichment of cell-targeting and population-specific aptamers by fluorescence-activated cell sorting. Angew Chem Int Ed Engl. 2008;47(28):5190-3.
[74] Klein R, Conway D, Parada LF, Barbacid M. The trkB tyrosine protein kinase gene codes for a second neurogenic receptor that lacks the catalytic kinase domain. Cell. 1990 May 18;61(4):647-56.
[75] Ni X, Castanares M, Mukherjee A, Lupold SE. Nucleic acid aptamers: clinical applications and promising new horizons. Curr Med Chem. 2011;18(27):4206-14.
[76] Amoresano A, Incoronato M, Monti G, Pucci P, de Franciscis V, Cerchia L. Direct interactions among Ret, GDNF and GFRalpha1 molecules reveal new insights into the assembly of a functional three-protein complex. Cell Signal. 2005 Jun;17(6):717-27.
[77] Ng EW, Shima DT, Calias P, Cunningham ET Jr, Guyer DR, Adamis AP. Pegaptanib, a targeted anti-VEGF aptamer for ocular vascular disease. Nat Rev Drug Discov. 2006 Feb;5(2):123-32.
[78] Esposito CL, Catuogno S, de Franciscis V, Cerchia L. New insight into clinical development of nucleic acid aptamers. Discov Med. 2011 Jun;11(61):487-96.
[79] Bates PJ, Laber DA, Miller DM, Thomas SD, Trent JO. Discovery and development of the G-rich oligonucleotide AS1411 as a novel treatment for cancer. Exp Mol Pathol. 2009 Jun;86(3):151-64.
[80] Girvan AC, Teng Y, Casson LK, Thomas SD, Jüliger S, Ball MW, Klein JB, Pierce WM Jr, Barve SS, Bates PJ. AGRO100 inhibits activation of nuclear factor-kappaB (NF-kappaB) by forming a complex with NF-kappaB essential modulator (NEMO) and nucleolin. Mol Cancer Ther. 2006 Jul;5(7):1790-9.
[81] Soundararajan S, Chen W, Spicer EK, Courtenay-Luck N, Fernandes DJ. The nucleolin targeting aptamer AS1411 destabilizes Bcl-2

messenger RNA in human breast cancer cells. Cancer Res. 2008 Apr 1;68(7):2358-65.
[82] Cerchia L, de Franciscis V. Targeting cancer cells with nucleic acid aptamers. Trends Biotechnol. 2010 Oct;28(10):517-25.
[83] Catuogno S, Esposito CL, de Franciscis V. Aptamer-Mediated Targeted Delivery of Therapeutics: An Update. Pharmaceuticals (Basel). 2016 Nov 3;9(4).
[84] Chen CH, Dellamaggiore KR, Ouellette CP, Sedano CD, Lizadjohry M, Chernis GA, Gonzales M, Baltasar FE, Fan AL, Myerowitz R, Neufeld EF. Aptamer-based endocytosis of a lysosomal enzyme. Proc Natl Acad Sci U S A. 2008 Oct14;105(41):15908-13.
[85] Hicke BJ, Stephens AW, Gould T, Chang YF, Lynott CK, Heil J, Borkowski S, Hilger CS, Cook G, Warren S, Schmidt PG. Tumor targeting by an aptamer. J Nucl Med. 2006 Apr;47(4):668-78.
[86] Tong GJ, Hsiao SC, Carrico ZM, Francis MB. Viral capsid DNA aptamer conjugates as multivalent cell-targeting vehicles. J Am Chem Soc. 2009 Aug12;131(31):11174-8.
[87] Cerchia L, Esposito CL, Camorani S, Catuogno S, Franciscis V. Coupling Aptamers to Short Interfering RNAs as Therapeutics. Pharmaceuticals (Basel). 2011Oct 27;4(11):1434-1449.
[88] Dhar S, Gu FX, Langer R, Farokhzad OC, Lippard SJ. Targeted delivery of cisplatin to prostate cancer cells by aptamer functionalized Pt(IV) prodrug-PLGA-PEG nanoparticles. Proc Natl Acad Sci U S A. 2008 Nov 11;105(45):17356-61.
[89] Ferreira CS, Cheung MC, Missailidis S, Bisland S, Gariépy J. Phototoxic aptamers selectively enter and kill epithelial cancer cells. Nucleic Acids Res. 2009 Feb;37(3):866-76.
[90] Neff CP, Zhou J, Remling L, Kuruvilla J, Zhang J, Li H, Smith DD, Swiderski P, Rossi JJ, Akkina R. An aptamer-siRNA chimera suppresses HIV-1 viral loads and protects from helper CD4(+) T cell decline in humanized mice. Sci Transl Med. 2011 Jan 19;3(66):66ra6.
[91] Kruspe S, Giangrande PH. Aptamer-siRNA Chimeras: Discovery, Progress, and Future Prospects. Biomedicines. 2017 Aug 9;5(3). pii: E45.
[92] Esposito CL, Cerchia L, Catuogno S, De Vita G, Dassie JP, Santamaria G, Swiderski P, Condorelli G, Giangrande PH, de Franciscis V. Multifunctional aptamer-miRNA conjugates for targeted cancer therapy. Mol Ther. 2014 Jun;22(6):1151-1163.
[93] Iaboni M, Russo V, Fontanella R, Roscigno G, Fiore D, Donnarumma E, Esposito CL, Quintavalle C, Giangrande PH, de Franciscis V, Condorelli G. Aptamer-miRNA-212 Conjugate Sensitizes NSCLC Cells to TRAIL. Mol Ther Nucleic Acids. 2016 Mar 8;5:e289.

[94] Catuogno S, Rienzo A, Di Vito A, Esposito CL, de Franciscis V. Selective delivery of therapeutic single strand antimiRs by aptamer-based conjugates. J Control Release. 2015 Jul 28;210:147-59.
[95] Esposito CL, Nuzzo S, Kumar SA, Rienzo A, Lawrence CL, Pallini R, Shaw L, Alder JE, Ricci-Vitiani L, Catuogno S, de Franciscis V. A combined microRNA-based targeted therapeutic approach to eradicate glioblastoma stem-like cells. J Control Release. 2016 Sep 28;238:43-57.
[96] Bagalkot V, Farokhzad OC, Langer R, Jon S. An aptamer-doxorubicin physical conjugate as a novel targeted drug-delivery platform. Angew Chem Int Ed Engl. 2006 Dec 11;45(48):8149-52.
[97] Hu Y, Duan J, Zhan Q, Wang F, Lu X, Yang XD. Novel MUC1 aptamer selectively delivers cytotoxic agent to cancer cells in vitro. PLoS One. 2012;7(2):e31970.
[98] Soontornworajit B, Wang Y. Nucleic acid aptamers for clinical diagnosis: cell detection and molecular imaging. Anal Bioanal Chem. 2011 Feb;399(4):1591-9.
[99] Hicke BJ, Stephens AW, Gould T, Chang YF, Lynott CK, Heil J, Borkowski S,Hilger CS, Cook G, Warren S, Schmidt PG. Tumor targeting by an aptamer. J Nucl Med. 2006 Apr;47(4):668-78.
[100] Levy-Nissenbaum E, Radovic-Moreno AF, Wang AZ, Langer R, Farokhzad OC. Nanotechnology and aptamers: applications in drug delivery. Trends Biotechnol. 2008 Aug;26(8):442-9.
[101] Dougherty CA, Cai W, Hong H. Applications of aptamers in targeted imaging: state of the art. Curr Top Med Chem. 2015;15(12):1138-52.
[102] Sun H, Tan W, Zu Y. Aptamers: versatile molecular recognition probes for cancer detection. Analyst. 2016 Jan 21;141(2):403-15.
[103] Zhu J, Li T, Hu J, Wang E. A novel dot-blot DNAzyme-linked aptamer assay for protein detection. Anal Bioanal Chem. 2010 Aug;397(7):2923-7.
[104] Tombelli S, Mascini M. Aptamers as molecular tools for bioanalytical methods. Curr Opin Mol Ther. 2009 Apr;11(2):179-88.
[105] Shin S, Kim IH, Kang W, Yang JK, Hah SS. An alternative to Western blot analysis using RNA aptamer-functionalized quantum dots. Bioorg Med Chem Lett. 2010 Jun 1;20(11):3322-5.
[106] Gold L, Ayers D, Bertino J, Bock C, Bock A, Brody EN, Carter J, Dalby AB, Eaton BE, Fitzwater T, Flather D, Forbes A, Foreman T, Fowler C, Gawande B, Goss M, Gunn M, Gupta S, Halladay D, Heil J, Heilig J, Hicke B, Husar G, Janjic N, Jarvis T, Jennings S, Katilius E, Keeney TR, Kim N, Koch TH, Kraemer S, Kroiss L, Le N, Levine D, Lindsey W, Lollo B, Mayfield W, Mehan M, Mehler R, Nelson SK,

Nelson M, Nieuwlandt D, Nikrad M, Ochsner U, Ostroff RM, Otis M, Parker T, Pietrasiewicz S, Resnicow DI, Rohloff J, Sanders G, Sattin S, Schneider D, Singer B, Stanton M, Sterkel A, Stewart A, Stratford S, Vaught JD, Vrkljan M, Walker JJ, Watrobka M, Waugh S, Weiss A, Wilcox SK, Wolfson A, Wolk SK, Zhang C, Zichi D.Aptamer-based multiplexed proteomic technology for biomarker discovery. PLoS One. 2010 Dec 7;5(12):e15004.
[107] Ivanov S, Liao SY, Ivanova A, Danilkovitch-Miagkova A, Tarasova N, Weirich G, Merrill MJ, Proescholdt MA, Oldfield EH, Lee J, Zavada J, Waheed A, Sly W, Lerman MI, Stanbridge EJ. Expression of hypoxia-inducible cell-surface transmembrane carbonic anhydrases in human cancer. Am J Pathol. 2001 Mar;158(3):905-19.
[108] Li Y, Wang H, Oosterwijk E, Tu C, Shiverick KT, Silverman DN, Frost SC. Expression and activity of carbonic anhydrase IX is associated with metabolic dysfunction in MDA-MB-231 breast cancer cells. Cancer Invest. 2009 Jul;27(6):613-23.
[109] Wenger RH, Kurtcuoglu V, Scholz CC, Marti HH, Hoogewijs D. Frequently asked
questions in hypoxia research. Hypoxia (Auckl). 2015 Sep 18;3:35-43.
[110] Supuran CT. Carbonic anhydrases: novel therapeutic applications for inhibitors and activators. Nat Rev Drug Discov. 2008 Feb;7(2):168-81.
[111] Semenza GL. Targeting HIF-1 for cancer therapy. Nat Rev Cancer. 2003 Oct;3(10):721-32.
[112] Vaupel P. The role of hypoxia-induced factors in tumor progression. Oncologist. 2004;9 Suppl 5:10-7.
[113] Parks SK, Chiche J, Pouyssegur J. pH control mechanisms of tumor survival and growth. J Cell Physiol. 2011 Feb;226(2):299-308.
[114] Parks SK, Chiche J, Pouyssegur J. pH control mechanisms of tumor survival and growth. J Cell Physiol. 2011 Feb;226(2):299-308.
[115] Samouilov A, Caia GL, Kesselring E, Petryakov S, Wasowicz T, Zweier JL. Development of a hybrid EPR/NMR coimaging system. Magn Reson Med. 2007 Jul;58(1):156-66.
[116] Oosterwijk E, Ruiter DJ, Hoedemaeker PJ, Pauwels EK, Jonas U, Zwartendijk J, Warnaar SO. Monoclonal antibody G 250 recognizes a determinant present in renal-cell carcinoma and absent from normal kidney. Int J Cancer. 1986 Oct15;38(4):489-94.
[117] Li Y, Wang H, Oosterwijk E, Selman Y, Mira JC, Medrano T, Shiverick KT, Frost SC. Antibody-specific detection of CAIX in breast and prostate cancers. BiochemBiophys Res Commun. 2009 Aug 28;386(3):488-92.

[118] Ahlskog JK, Schliemann C, Mårlind J, Qureshi U, Ammar A, Pedley RB, Neri D. Human monoclonal antibodies targeting carbonic anhydrase IX for the molecular imaging of hypoxic regions in solid tumours. Br J Cancer. 2009 Aug 18;101(4):645-57.
[119] Zhu H, Zhang L, Liu Y, Zhou Y, Wang K, Xie X, Song L, Wang D, Han C, Chen Q. Aptamer-PEG-modified Fe(3)O(4)@Mn as a novel T1- and T2- dual-model MRI contrast agent targeting hypoxia-induced cancer stem cells. Sci Rep. 2016 Dec 15;6:39245.
[120] Rong Y, Chen H, Zhou XF, Yin CQ, Wang BC, Peng CW, Liu SP, Wang FB.Identification of an aptamer through whole cell-SELEX for targeting high
metastatic liver cancers. Oncotarget. 2016 Feb 16;7(7):8282-94.
[121] Wang G, Liu J, Chen K, Xu Y, Liu B, Liao J, Zhu L, Hu X, Li J, Pu Y, Zhong W, Fu T, Liu H, Tan W. Selection and characterization of DNA aptamer against glucagon receptor by cell-SELEX. Sci Rep. 2017 Aug 3;7(1):7179.